

UBSEA: A UNIFIED COMMUNITY DETECTION FRAMEWORK

BY XIANCHENG LIN AND HAO CHEN

University of California, Davis

Detecting communities in networks and graphs is an important task across many disciplines such as statistics, social science and engineering. There are generally three different kinds of mixing patterns for the case of two communities: assortative mixing, disassortative mixing and core-periphery structure. Modularity optimization is a classical way for fitting network models with communities. However, it can only deal with assortative mixing and disassortative mixing when the mixing pattern is known and fails to discover the core-periphery structure. In this paper, we extend modularity in a strategic way and propose a new framework based on **Unified Bigroups Standardized Edge-count Analysis (UBSea)**. It can address all the formerly mentioned community mixing structures. In addition, this new framework is able to automatically choose the mixing type to fit the networks. Simulation studies show that the new framework has superb performance in a wide range of settings under the stochastic block model and the degree-corrected stochastic block model. We show that the new approach produces consistent estimate of the communities under a suitable signal-to-noise-ratio condition, for the case of a block model with two communities, for both undirected and directed networks. The new method is illustrated through applications to several real-world datasets.

1. Introduction. Network data analysis attracts attention across many disciplines such as sociology, statistics, computer science and biology. One of the fundamental tasks in network data analysis is detecting communities/clusters. Many algorithms have been proposed for fitting network models with communities. A standard framework for studying community detection in a statistical setting is the Stochastic Block Model (SBM) proposed in [Holland, Laskey and Leinhardt \(1983\)](#). For a network with N nodes, given its $N \times N$ adjacency matrix \mathbf{A} , this model assumes that the true node labels $\mathbf{c} = (c_1, \dots, c_N) \in \{1, \dots, K\}^N$ are drawn independently from the multinomial distribution with proportion parameter $\boldsymbol{\pi} = (\pi_1, \dots, \pi_K)$, where $\pi_i > 0$ for all i , and K is the number of communities, assumed known. Conditional on the labels assignment \mathbf{c} , the edge variables A_{ij} independently follows Bernoulli distribution with

$$(1) \quad \mathbb{E}[A_{ij}|\mathbf{c}] = P_{c_i c_j},$$

where $\mathbf{P} = [P_{ab}]$ is a $K \times K$ connectivity matrix. The task of community detection is then to infer the node labels \mathbf{c} from the adjacency matrix \mathbf{A} , and often involves estimating $\boldsymbol{\pi}$ and \mathbf{P} . In this paper, we will consider the case where $K = 2$, i.e., two different communities.

There are many extensions of the block model, such as the Mixed Membership Stochastic Block Model in [Airoldi et al. \(2008\)](#), the Weighted Stochastic Block Model in [Peixoto \(2018\)](#), to name but a few. One notable extension is the Degree-Corrected Stochastic Block Model (DCSBM) ([Karrer and Newman, 2011](#)). It removes the unrealistic constraint of the same expected degree for all nodes within the same community in SBM by replacing (1)

MSC2020 subject classifications: Primary 62R99; secondary 91C20.

Keywords and phrases: assortative mixing, disassortative mixing, core-periphery structure, directed network, penalized likelihood, social network.

with $\mathbb{E}[A_{ij}|c] = \theta_i \theta_j P_{c_i c_j}$, where θ_i 's are node degree parameters which satisfy an identifiability constraint such as $\mathbb{E}[\theta_i] = 1$ or $\theta_{\max} = 1$. Researchers tend to replace the Bernoulli distribution for A_{ij} by the Poisson distribution for the ease of technical derivations, which is in fact a good approximation for a range of networks; see [Karrer and Newman \(2011\)](#).

For the case of two communities, there are generally three types of mixing patterns under SBM for undirected networks. In the most commonly studied case, P_{11} and P_{22} are both larger than P_{12} , meaning that the probability for connections within communities are larger than the probability between communities. This choice gives us the traditional community structure called the assortative mixing ([Newman, 2002, 2003a,b](#)). To the opposite of the assortative mixing is the disassortative choice where P_{11} and P_{22} are both smaller than P_{12} , which means nodes are more likely to connect with nodes in the different communities. This disassortative mixing, commonly found in biological, technological networks and other fields, has received a modest amount of attention in the literature; see [Newman and Leicht \(2007\)](#); [Moore et al. \(2011\)](#). There is, however, a third kind of mixing pattern in which $P_{11} > P_{12} > P_{22}$ (or $P_{22} > P_{12} > P_{11}$), which is called the core-periphery structure; see [Zhang, Martin and Newman \(2015\)](#). Already in late 1990s, sociologists noticed that the core-periphery structure exhibited in a number of social networks; see [Borgatti and Everett \(2000\)](#). Without loss of generality, we can assume P_{11} to be the largest of the three probabilities. Community one is then called the core and community two the periphery. In the core-periphery structure, edges are most likely to be within the core, least probable within the periphery, and modest number of edges between core and periphery.

Many algorithms have been proposed for fitting networks with community structures mentioned above, respectively. There are in general three categories of traditional methods: Spectral methods, likelihood-based methods and modularity-based methods. Spectral methods estimate the communities using the graph eigenvectors and are usually computationally fast; see [Von Luxburg \(2007\)](#). Spectral methods are known to suffer from inconsistency in sparse graphs ([Krzakala et al., 2013](#)) and are often sensitive to outliers ([Cai and Li, 2015](#)). Profile likelihood maximization methods, for instance, [Wang and Bickel \(2017\)](#), are often computationally intractable since they need to estimate a large number of parameters. One notable exception is the CPL method in [Amini et al. \(2013\)](#), which is efficient in solving large scale sparse networks. Methods based on modularity optimization have been found to produce excellent results. In general, modularity maximization targets at assortative mixing patterns; see [Newman \(2002\)](#); [Newman and Girvan \(2004\)](#); [Newman \(2006a\)](#). Modularity minimization, on the contrary, discovers the disassortative mixing pattern; see [Newman \(2006b\)](#). However, modularity fails to discover core-periphery structure. Researchers in modularity domain thereafter turn to likelihood methods to handle the core-periphery structure, making the modularity based community detection framework incomplete. Also, they most of the time only tested the performance under the simple stochastic block model; see [Zhang, Martin and Newman \(2015\)](#). It is worth pointing out that all these popular methods mentioned above are mainly designed for undirected networks and often require converting the directed graph to the undirected one, which in a sense, changes the graph information carried by the edges; see [Malliaros and Vazirgiannis \(2013\)](#) for a review. The most significant problem is that none of them provide a satisfying framework to include all the formerly mentioned mixing patterns simultaneously. Moreover, people usually focus on one specific mixing pattern, mostly assortative mixing, to fit the network observation. Therefore, none of them can assess which mixing pattern is the most significant among the three mixing patterns.

The question remains, can we build a unified community detection framework to include all the following community structures and network types: assortative mixing, disassortative mixing, core-periphery structure, undirected networks and directed networks. The answer is surprisingly YES by revisiting the original definition of modularity. We extend modularity

discussed in Newman (2006a) in a strategic way and propose a novel UBSea community detection framework which contains two closely related standardized clustering statistic Z_w and Z_d , which will be maximized or minimized at the true clustering labels up to a permutation in high probability under proper conditions. The statistic Z_d , proposed in Chen and Friedman (2017), was originally designed to overcome the difficulty in two-sample test affected by the curse of dimensionality. Later, another edge-count statistic, the weighted edge-count statistic Z_w , was proposed in Chen, Chen and Su (2018). In the two-sample test region, the statistic Z_w focuses on the location alternative and the statistic Z_d exhibits high power under a wide range of alternatives but is especially powerful in the scale alternative. Here in the community detection region, we will see that, these two statistics play similar roles as in the two-sample test setting. The community detection performance based on the statistic Z_w is similar to traditional community detection methods such as modularity methods or spectral clustering methods. The statistic Z_w is mainly used to examine the assortative mixing and disassortative mixing patterns, while Z_d mostly focus on the core-periphery structure. But they do have certain overlap and can both be powerful in a wide range of settings. As a result, when combined together, they form the foundation of our UBSea community detection framework. We prove that, the statistic Z_w provides almost exact recovery of the communities, in the sense the misclustering fraction, up to a permutation, goes to zero, under a certain condition of the signal-to-noise ratio (SNR). When the model is the symmetric stochastic block model with two communities, this condition on the connectivity matrix is equivalent to the one derived in Amini et al. (2013). The statistic Z_d provides almost exact recovery estimates of the communities, under a similar condition of SNR, for the case of two communities. We also prove exact recovery, in the sense that the number of misclustering nodes goes to zero, under slightly stronger conditions.

In order to build a complete framework, the last step is how to choose among Z_w , Z_d and other possibly related quantities in a statistical way. First, if the network follows the SBM, we found a γ - τ criterion, which originates from the above mentioned consistency results, can be utilized to choose among those three mixing patterns. In a more general setting where the DCSBM better fits the network, we adopt the idea in Wang and Bickel (2017), in which they use the penalized likelihood to solve the problem of estimating the proper number of communities under SBM and DCSBM. We view the heterogeneity of the degree parameters θ 's estimated by the given mixing pattern as the model complexity and thereafter develop a penalized likelihood criterion to choose among those three mixing patterns. We found that the penalized likelihood criterion to be more powerful than the γ - τ criterion in the DCSBM case.

Besides, our novel UBSea community detection framework is suitable for both undirected and directed networks. The problem of network community detection has mainly been considered and studied for the case of undirected networks. A huge number of diverse algorithms have been proposed for the undirected setting, involving contributions from the fields of computer science, statistics, social science, physics and biology (Aggarwal and Wang, 2010). Nevertheless, numerous graph data in several applications are by nature directed. The problem of community detection in directed networks is considered to be a more challenging task as compared to the undirected case; see the review Malliaros and Vazirgiannis (2013). Traditional undirected methods convert the directed graphs to undirected graphs as the first step, which surely changes the information carried by the edges. While our framework can be applied to directed networks directly to fully use the direction information. Simulation results show that our UBSea framework is consistently powerful for both undirected and directed networks.

The rest of paper is organized as follows. We present the new method and consistency results in Section 2. The numerical performance of the methods is demonstrated in Section

3. Section 4 states the unified community detection framework. We test the new framework on several real world datasets in Section 5. Section 6 concludes with discussion. Section 7 provides the main steps of the proof for consistency results.

2. Proposed method and theory. In this section, we first revisit the original definition of modularity and explain its intuition, as well as reasons for us to extend it. Then we introduce two statistics R_w and R_d , which will be of central interest in our paper. We calculate their expectations and variances under the permutation null distribution. We show that the standardized versions of R_w and R_d , called Z_w and Z_d can be used as community detection criteria. We determine the requirements of the growth rate on the connectivity matrix, in order to achieve almost exact recovery (weak consistency) and exact recovery (strong consistency), respectively, in the sense the misclustering fraction (weak consistency) or misclustering number (strong consistency) decay to 0 as node size increases, for the case of two communities. We state the results in this section and defer the consistency proofs in Section 7 and all other proofs in Supplementary Material [Lin and Chen \(2023\)](#).

2.1. *Revisit Modularity.* There are many different forms of modularity. We here analyze the original form in [Newman \(2006a\)](#):

$$\begin{aligned}
 (2) \quad Q &= \sum_{i,j} \left(A_{ij} - \frac{k_i k_j}{2m} \right) \frac{(s_i s_j + 1)}{2} \\
 &= (\text{number of edges within communities}) - (\text{expected number of such edges}) \\
 &= (R - \mathbb{E}R),
 \end{aligned}$$

where $s_i = +1$ if vertex i belongs to group 1 and $s_i = -1$ if it belongs to group 2, k_i, k_j are node degrees and m is the total number of edges in the network. Let R_1 be the edges inside community 1 and R_2 be the edges inside community 2, then $R = R_1 + R_2$ is the edges inside the same community. The choice of the ‘‘expected number’’ of edges is essentially equivalent to choosing a ‘‘null model’’ against which to compare the network. The null model behind modularity is close to the configuration model, where the edges are placed at random resulting in the network follows some pre-given degree distribution. Intuitively, modularity measures the total deviation of edges inside each community from its expected number under the chosen ‘‘null model’’. Therefore, when there are two assortative communities, the edges inside them will both be larger than the expected number and modularity maximization is then able to capture this structure. On the contrary, when there are two disassortative communities, the edges inside them are both smaller than the expected number, hence modularity minimization is suitable in this case. However, in the core-periphery case, the deviation measurement inside the core is positive while the deviation measurement inside the periphery is negative, hence they cancel each other out when summed up. Therefore, modularity maximization and minimization could not recognize the core-periphery structure. To sum up, the choice of the original modularity has the following drawbacks: First, it cannot deal with core-periphery structure as explained above. Second, traditionally, people maximize modularity to find assortative communities. While minimizing modularity can find disassortative communities, it is then not clear when to maximize or minimize it. Third, introducing the degree parameter k_i then arising an issue about whether to use k^{in} or k^{out} in directed graphs; see [Leicht and Newman \(2008\)](#) for a discussion. Last, researchers found that the normalizing term $\frac{1}{2m}$ might not work well under some common settings and they proposed to use a tuning parameter λ to replace $\frac{1}{2m}$ in (2) ([Reichardt and Bornholdt, 2006](#); [Fortunato and Barthelemy, 2007](#)), which abandoned the interpretability of the null model. With these in mind, instead of sacrificing the interpretability of modularity to perform modifications, our idea is to put

modularity back to its general class, try different expectations, generalize R in the following way:

- We adopt a different $\mathbb{E}A_{ij}$: The expectation under the permutation distribution, i.e., the null model is that there is only one community.
- We generalize $R = R_1 + R_2$ to be $\tilde{R} = aR_1 + bR_2$, where a and b could be functions of the community sizes.

2.2. *Analysis of Z_w and Z_d .* We use (G, E) to denote the graph and the set of edges. When the graph is directed, $(i, j) \in E$ means that there is an edge pointing from node i to node j . When the graph is undirected, $(i, j) \equiv (j, i)$, and $(i, j) \in E$ means there is an edge between nodes i and j . We assume there is no self-loop in the graph. Let \mathbf{x} be an N -length vector of 0's and 1's.

$$R_1(\mathbf{x}) = \sum_{(i,j) \in E} I_{x_i=x_j=1}, \quad R_2(\mathbf{x}) = \sum_{(i,j) \in E} I_{x_i=x_j=0}.$$

The vector \mathbf{x} divides the observations into two communities: 1's (Community 1) and 0's (Community 2). Let $m_{\mathbf{x}} = \sum_{i=1}^N x_i$ be the number of vertices in the first community implied by \mathbf{x} , and $n_{\mathbf{x}} = N - m_{\mathbf{x}}$ be the number of vertices in the second community. Also, Let \mathbf{x}^* represents the true community label, and there are m 1's and n 0's in \mathbf{x}^* , where m and n are the true community sizes. Let $\mathbf{P} = \begin{bmatrix} P_{11} & P_{12} \\ P_{21} & P_{22} \end{bmatrix}$ be the connectivity matrix, where P_{ij} represents the probability of edge between community i and community j . There are a number of reasonable choices for a and b in the definition of \tilde{R} to generalize modularity. We here present two candidates named R_d and R_w to serve as an example to show the behavior of different choices through the analysis under stochastic block model. We will see that R_d plays as the proof basis for other more complicated generalizations and R_w is an example of taking consideration of the community sizes. To be more specific, define $R_w(\mathbf{x})$ and $R_d(\mathbf{x})$ and their normalized versions $Z_w(\mathbf{x})$ and $Z_d(\mathbf{x})$ to be the following terms:

$$Z_w(\mathbf{x}) = \frac{R_w(\mathbf{x}) - \mu_w(\mathbf{x})}{\sigma_w(\mathbf{x})}, \quad R_w(\mathbf{x}) = \frac{n_{\mathbf{x}} - 1}{N - 2} R_1(\mathbf{x}) + \frac{m_{\mathbf{x}} - 1}{N - 2} R_2(\mathbf{x}),$$

$$Z_d(\mathbf{x}) = \frac{R_d(\mathbf{x}) - \mu_d(\mathbf{x})}{\sigma_d(\mathbf{x})}, \quad R_d(\mathbf{x}) = R_1(\mathbf{x}) - R_2(\mathbf{x}),$$

where $\mu_w(\mathbf{x})$, $\sigma_w(\mathbf{x})$, $\mu_d(\mathbf{x})$, $\sigma_d(\mathbf{x})$ are normalizing terms. Their expressions can be obtained through similar treatments in [Chen and Friedman \(2017\)](#) and [Liu and Chen \(2022\)](#) and are provided below.

LEMMA 2.1. *The expectation and variance of $R_w(\mathbf{x})$ and $R_d(\mathbf{x})$ on the **directed** graph (G, E) under permutation null are:*

$$\mu_w(\mathbf{x}) \triangleq \mathbb{E}(R_w(\mathbf{x})) = \frac{(m_{\mathbf{x}} - 1)(n_{\mathbf{x}} - 1)}{(N - 1)(N - 2)} |G|,$$

$$\sigma_w^2(\mathbf{x}) \triangleq \text{Var}(R_w(\mathbf{x})) = \frac{m_{\mathbf{x}} n_{\mathbf{x}} (m_{\mathbf{x}} - 1)(n_{\mathbf{x}} - 1)}{N(N - 1)(N - 2)^2} \left(|G| + q_1 - \frac{|G|^2}{N - 1} + \frac{q_2}{N - 3} \right),$$

$$\mu_d(\mathbf{x}) \triangleq \mathbb{E}(R_d(\mathbf{x})) = \frac{m_{\mathbf{x}} - n_{\mathbf{x}}}{N} |G|,$$

$$\sigma_d^2(\mathbf{x}) \triangleq \text{Var}(R_d(\mathbf{x})) = \frac{m_{\mathbf{x}} n_{\mathbf{x}}}{N(N - 1)} \left(|G| + q_1 + |G|^2 \frac{N - 4}{N} - q_2 \right),$$

where $|G|, q_1, q_2$ are quantities on the graph (G, E) :

$$|G| = \sum_{i=1}^N \sum_{j=1}^N \mathbb{1}_{\{(i,j) \in E\}}, \quad q_1 = \sum_{i=1}^N \sum_{j \in D_i^s} \mathbb{1}_{\{(i,j) \in E\}},$$

$$q_2 = |G|^2 - |G| - q_1 - 2 \sum_{i=1}^N \sum_{j \in D_i^s} k_j^{\text{out}} - \sum_{i=1}^N k_i^{\text{out}} (k_i^{\text{out}} - 1) - \sum_{i=1}^N k_i^{\text{in}} (k_i^{\text{in}} - 1).$$

Here, D_i^s is the set of vertices that point toward vertex i , k_i^{in} is the cardinality of set D_i^s , or the in-degree of vertex i , k_i^{out} is the out-degree of vertex i .

LEMMA 2.2. The expectation and variance of $R_w(\mathbf{x})$ and $R_d(\mathbf{x})$ on the **undirected** graph (\ddot{G}, \ddot{E}) under permutation null are:

$$\mu_w(\mathbf{x}) \triangleq \mathbb{E}(R_w(\mathbf{x})) = \frac{(m_{\mathbf{x}} - 1)(n_{\mathbf{x}} - 1)}{(N - 1)(N - 2)} |\ddot{G}|,$$

$$\sigma_w^2(\mathbf{x}) \triangleq \text{Var}(R_w(\mathbf{x})) = \frac{m_{\mathbf{x}} n_{\mathbf{x}} (m_{\mathbf{x}} - 1)(n_{\mathbf{x}} - 1)}{N(N - 1)(N - 2)^2} \left(|\ddot{G}| - \frac{|\ddot{G}|^2}{N - 1} + \frac{\ddot{q}_2}{N - 3} \right),$$

$$\mu_d(\mathbf{x}) \triangleq \mathbb{E}(R_d(\mathbf{x})) = \frac{m_{\mathbf{x}} - n_{\mathbf{x}}}{N} |\ddot{G}|,$$

$$\sigma_d^2(\mathbf{x}) \triangleq \text{Var}(R_d(\mathbf{x})) = \frac{m_{\mathbf{x}} n_{\mathbf{x}}}{N(N - 1)} \left(|\ddot{G}| + |\ddot{G}|^2 \frac{N - 4}{N} - \ddot{q}_2 \right),$$

where $|\ddot{G}|, \ddot{q}_2$ are quantities on the graph (\ddot{G}, \ddot{E}) :

$$|\ddot{G}| = \sum_{i=1}^N \sum_{j=1}^i \mathbb{1}_{\{(i,j) \in \ddot{E}\}}, \quad \ddot{q}_2 = |\ddot{G}|^2 - |\ddot{G}| - \sum_{i=1}^N k_i (k_i - 1).$$

Here, k_i is the degree of vertex i .

Lemma 2.1 and Lemma 2.2 can be proved by combinatorial analysis similar in [Chen and Friedman \(2017\)](#) and [Liu and Chen \(2022\)](#). The expectations are relatively simple due to the linearity of expectation. For the variances, if the graph is directed, we have to figure out the number of possible configurations of pairs of edges plotted in Figure 1. For undirected graphs, the treatment is slightly easier as the number of configurations to be considered is less.

Following the treatment in [Chen and Lin \(2023\)](#), we can define $\mathbb{E}_2(\cdot)$ to be the expectation under the two communities SBM with the connectivity matrix \mathbf{P} . We let

$$R_{d,c}^P(\mathbf{x}) = \mathbb{E}_2(R_d(\mathbf{x}) - \mu_d(\mathbf{x})), \quad R_{w,c}^P(\mathbf{x}) = \mathbb{E}_2(R_w(\mathbf{x}) - \mu_w(\mathbf{x})).$$

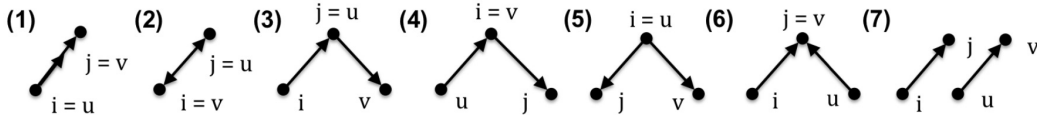


FIG 1. Seven possible configurations of two edges $(i, j), (u, v)$ randomly chosen, with replacement, from a directed graph: (1) two edges degenerate into one; (2) two opposite edges; (3)-(6) four different configurations with the two edges sharing one node; (7) two edges without any node sharing.

For directed graphs, given the label assignment \mathbf{x} and true label \mathbf{x}^* , suppose there are $\Delta_1 \in [0, m]$ observations in community 1 placed into community 2, and $\Delta_2 \in [0, n]$ observations in community 2 placed into community 1. The associated sizes of the two communities of assignment \mathbf{x} are

$$m_{\mathbf{x}} = m - \Delta_1 + \Delta_2, \quad n_{\mathbf{x}} = n - \Delta_2 + \Delta_1.$$

Then,

$$\mathbb{E}_2(R_1(\mathbf{x})) = (m - \Delta_1)(m - \Delta_1 - 1)P_{11} + (m - \Delta_1)\Delta_2(P_{12} + P_{21}) + \Delta_2(\Delta_2 - 1)P_{22},$$

$$\mathbb{E}_2(R_2(\mathbf{x})) = (n - \Delta_2)(n - \Delta_2 - 1)P_{22} + (n - \Delta_2)\Delta_1(P_{12} + P_{21}) + \Delta_1(\Delta_1 - 1)P_{11},$$

$$\mathbb{E}_2(\mu_d(\mathbf{x})) = \frac{(m - n) - 2(\Delta_1 - \Delta_2)}{N} (m(m - 1)P_{11} + mn(P_{12} + P_{21}) + n(n - 1)P_{22}),$$

$$\begin{aligned} \mathbb{E}_2(\mu_w(\mathbf{x})) &= \frac{(m - \Delta_1 + \Delta_2 - 1)(n - \Delta_2 + \Delta_1 - 1)}{(N - 1)(N - 2)} (m(m - 1)P_{11} + mn(P_{12} + P_{21}) \\ &\quad + n(n - 1)P_{22}), \end{aligned}$$

$$\mathbb{E}_2(R_w(\mathbf{x}) - \mu_w(\mathbf{x}))$$

$$\begin{aligned} &= \frac{1}{N - 2} \{ P_{11}((n - \Delta_2 + \Delta_1 - 1)(m - \Delta_1)(m - \Delta_1 - 1) \\ &\quad + (m - \Delta_1 + \Delta_2 - 1)\Delta_1(\Delta_1 - 1)) + P_{22}((n - \Delta_2 + \Delta_1 - 1)\Delta_2(\Delta_2 - 1) \\ &\quad + (m - \Delta_1 + \Delta_2 - 1)(n - \Delta_2)(n - \Delta_2 - 1)) \\ &\quad + (P_{12} + P_{21})((m - \Delta_1)\Delta_2(n - \Delta_2 + \Delta_1 - 1) + (n - \Delta_2)\Delta_1(m - \Delta_1 + \Delta_2 - 1) \\ &\quad - \frac{(m - \Delta_1 + \Delta_2 - 1)(n - \Delta_2 + \Delta_1 - 1)}{(N - 1)} (m(m - 1)P_{11} + mn(P_{12} + P_{21}) \\ &\quad + n(n - 1)P_{22})) \} \\ &= \frac{mn(m - 1)(n - 1)}{(N - 1)(N - 2)} (P_{11} + P_{22} - P_{12} - P_{21}) \\ &\quad \times \left(1 + \frac{\Delta_1^2}{m(m - 1)} + \frac{\Delta_2^2}{n(n - 1)} - \frac{(2m - 1)\Delta_1}{m(m - 1)} - \frac{(2n - 1)\Delta_2}{n(n - 1)} + \frac{2\Delta_1\Delta_2}{mn} \right), \end{aligned}$$

$$\mathbb{E}_2(R_d(\mathbf{x}) - \mu_d(\mathbf{x}))$$

$$\begin{aligned} &= P_{11}((m - \Delta_1)(m - \Delta_1 - 1) - \Delta_1(\Delta_1 - 1)) \\ &\quad + P_{22}(\Delta_2(\Delta_2 - 1) - (n - \Delta_2)(n - \Delta_2 - 1)) \\ &\quad + (P_{12} + P_{21})((m - \Delta_1)\Delta_2 - (n - \Delta_2)\Delta_1) \\ &\quad - \frac{(m - n) - 2(\Delta_1 - \Delta_2)}{N} (m(m - 1)P_{11} + mn(P_{12} + P_{21}) + n(n - 1)P_{22}) \\ &= \frac{mn}{m + n} (2(m - 1)P_{11} - 2(n - 1)P_{22} - (m - n)(P_{12} + P_{21})) \left(1 - \frac{\Delta_1}{m} - \frac{\Delta_2}{n} \right). \end{aligned}$$

The expressions of them for undirected graphs can be derived almost identically and are omitted here. Now, we are ready to introduce the optimization results for $R_{w,c}^P(\mathbf{x})$ and $R_{d,c}^P(\mathbf{x})$.

THEOREM 2.3. *Let \mathbf{x}^* , m , n denote the true community label and the corresponding number of vertices in community 1's and community 0's, respectively:*

- *When $2(m-1)P_{11} - 2(n-1)P_{22} - (m-n)(P_{12} + P_{21}) \neq 0$, $R_{d,c}^P(\mathbf{x})$ and $R_{d,c}^P(\mathbf{x})/\sigma_d(\mathbf{x})$ are maximized at $\mathbf{x} = \mathbf{x}^*$ or $\mathbf{x} = 1 - \mathbf{x}^*$.*
- *When $P_{11} + P_{22} - P_{12} - P_{21} > 0$, $R_{w,c}^P(\mathbf{x})$ and $R_{w,c}^P(\mathbf{x})/\sigma_w(\mathbf{x})$ are maximized at $\mathbf{x} = \mathbf{x}^*$ or $\mathbf{x} = 1 - \mathbf{x}^*$.*
- *When $P_{11} + P_{22} - P_{12} - P_{21} < 0$, $R_{w,c}^P(\mathbf{x})$ and $R_{w,c}^P(\mathbf{x})/\sigma_w(\mathbf{x})$ are minimized at $\mathbf{x} = \mathbf{x}^*$ or $\mathbf{x} = 1 - \mathbf{x}^*$.*

REMARK 2.4. The condition for $R_{d,c}^P(\mathbf{x})$ can be approximated by $\frac{m}{n} = \frac{P_{12} + P_{21} - 2P_{22}}{P_{12} + P_{21} - 2P_{11}}$. When $m = n$, and the connectivity matrix is symmetric, this is to say $P_{11} = P_{22}$.

The proof of Theorem 2.3 follows directly from Theorem 1 in [Chen and Lin \(2023\)](#) and is provided in Supplementary Material ([Lin and Chen, 2023](#)). For simplicity, in the following we denote $R_{d,c}^P(\mathbf{x})/\sigma_d(\mathbf{x})$, $R_{w,c}^P(\mathbf{x})/\sigma_w(\mathbf{x})$ as $Z_d^P(\mathbf{x})$ and $Z_w^P(\mathbf{x})$, respectively. The optimization properties of $Z_w^P(\mathbf{x})$ and $Z_d^P(\mathbf{x})$ are crucial in establishing the consistency results for $Z_w(\mathbf{x})$ and $Z_d(\mathbf{x})$ in Section 2.3. Additionally, it is noteworthy that these conditions, derived from $Z_d^P(\mathbf{x})$ and $Z_w^P(\mathbf{x})$, are often to be effective for $Z_d(\mathbf{x})$ and $Z_w(\mathbf{x})$ in practice.

2.3. Consistency Result. Denote χ_N as the collection of $\{0, 1\}^N$. Denote the true label as $\mathbf{x}^* \in \chi_N$ with the community sizes $m \geq 2$ and $n \geq 2$, $N = m + n$ is the total node size. For a label $\mathbf{x} \in \chi_N$ with $\Delta_1 \in [0, m]$ observations in community 1 placed into community 2, and $\Delta_2 \in [0, n]$ observations in community 2 placed into community 1, then $m_{\mathbf{x}} = m - \Delta_1 + \Delta_2$, $n_{\mathbf{x}} = n - \Delta_2 + \Delta_1$. Let $\delta_1 = \frac{\Delta_1}{m} \in [0, 1]$, $\delta_2 = \frac{\Delta_2}{n} \in [0, 1]$ be the corresponding misclustering proportion. Besides, we define $a_n = o(b_n)$ or $a_n \ll b_n$ as a_n is dominated by b_n asymptotically i.e. $\lim_{n \rightarrow \infty} \frac{a_n}{b_n} = 0$, $a_n = O(b_n)$ or $a_n \asymp b_n$ as a_n is bounded both above and below by b_n asymptotically, and $a_n \lesssim b_n$ as a_n is bounded above by b_n (up to constant factor) asymptotically.

We analyze the consistency property under a block model as the number of nodes in the graph G grows. We condition on the community labels $\{c_i\}$, that is, we treat them as deterministic unknown parameters. Recall that for the block model, we assume all the entries in the adjacency matrix are drawn independently from Bernoulli distribution, that is,

$$A_{ij} \sim \text{Ber}(P_{c_i c_j}) \quad \text{for all } i, j.$$

where $c_i \in \{1, 2\}$ corresponding to community 1 and community 2. Here in the proof, we assume that diagonal entries of the adjacency matrix are also drawn randomly (i.e., we allow for self-loops as valid with-community edges). This is convenient in the analysis with minor effect on the results. Our approach is to prove consistency result for the SBM model, with the connectivity matrix of the form:

$$\mathbf{P} = \begin{pmatrix} P_{11} & P_{12} \\ P_{21} & P_{22} \end{pmatrix}.$$

Here, all P_{ij} 's depend on N and can change with N at different rates. Note that we don't have additional restrictions on the connectivity matrix. This is different from the literature where they usually consider the Symmetric Stochastic Block Model (SSBM), where the diagonal and off-diagonal elements of the connectivity matrix are the same, such as [Amini et al. \(2013\)](#). We will see that, our consistency requirement is more generic and is equivalent to the condition on the connectivity matrix derived in [Amini et al. \(2013\)](#) when the model is SSBM.

The notion of consistency of community detection as the number of nodes grows was introduced in [Bickel and Chen \(2009\)](#). They defined a community detection criterion Q to be consistent if the node labels obtained by maximizing the criterion, $\hat{\mathbf{c}} = \arg \max_{\mathbf{x}} Q(\mathbf{x})$, satisfy

$$(3) \quad P[\hat{\mathbf{c}} = \mathbf{c}] \rightarrow 1 \quad \text{as } N \rightarrow \infty.$$

Strictly speaking, this definition suffers from an identifiability issue. Because we can always do communities permutation. Thus, a better way to define consistency is to replace the equality $\hat{\mathbf{c}} = \mathbf{c}$ with the requirement that $\hat{\mathbf{c}}$ and \mathbf{c} belong to the same equivalence class of label permutations. For simplicity of notation, we still write $\hat{\mathbf{c}} = \mathbf{c}$ below.

The notion of consistency in [Bickel and Chen \(2009\)](#) is very strong, since it requires asymptotically no errors. Instead, we can also define the following notion of consistency,

$$(4) \quad \forall \varepsilon > 0 \quad \mathbb{P} \left[\left(\frac{1}{N} \sum_{i=1}^N \mathbb{I}(\hat{c}_i \neq c_i) \right) < \varepsilon \right] \rightarrow 1 \quad \text{as } N \rightarrow \infty.$$

where equality is also interpreted to mean labels in the same equivalence class with respect to label permutations.

Consistency pattern (4) was called weak consistency in [Zhao, Levina and Zhu \(2012\)](#), in the sense that the misclustering fraction goes to zero as the graph node size increases. Consistency pattern (3) is the strong consistency used in [Karrer and Newman \(2011\)](#), which means the clustering label is the same as the true label with high probability as the graph node size increases. By defining $\gamma_N^2 = \frac{(2\pi_1 P_{11} - 2\pi_2 P_{22} - (\pi_1 - \pi_2)(P_{12} + P_{21}))^2}{\max(P)}$, $\tau_N^2 = \frac{(P_{11} + P_{22} - P_{12} - P_{21})^2}{\max(P)}$, we will present both weak and strong consistency results for our method.

THEOREM 2.5 (Weak Consistency). *Under the SBM,*

- If $N\gamma_N^2 \rightarrow \infty$, then $\hat{\mathbf{c}} = \arg \max_{\mathbf{x}} Z_d(\mathbf{x})$ is weakly consistent under the assumption that there exists a sequence α_N with $\alpha_N \rightarrow 0$ and $\alpha_N N\gamma_N^2 \rightarrow \infty$ such that

$$(5) \quad N e^{-\alpha_N N\gamma_N^2} < m_{\mathbf{x}}, n_{\mathbf{x}} < N(1 - e^{-\alpha_N N\gamma_N^2}),$$

where $m_{\mathbf{x}}, n_{\mathbf{x}}$ are the corresponding group sizes of $\arg \max_{\mathbf{x}} Z_d(\mathbf{x})$.

- If $N\tau_N^2 \rightarrow \infty$ and $P_{11} + P_{22} - P_{12} - P_{21} > 0$, then $\hat{\mathbf{c}} = \arg \max_{\mathbf{x}} Z_w(\mathbf{x})$ is weakly consistent under the assumption that there exists a sequence β_N with $\beta_N \rightarrow 0$ and $\beta_N N\tau_N^2 \rightarrow \infty$ such that

$$(6) \quad N e^{-\beta_N N\tau_N^2} < m_{\mathbf{x}}, n_{\mathbf{x}} < N(1 - e^{-\beta_N N\tau_N^2}),$$

where $m_{\mathbf{x}}, n_{\mathbf{x}}$ are the corresponding group sizes of $\arg \max_{\mathbf{x}} Z_w(\mathbf{x})$.

- If $N\tau_N^2 \rightarrow \infty$ and $P_{11} + P_{22} - P_{12} - P_{21} < 0$, then $\hat{\mathbf{c}} = \arg \min_{\mathbf{x}} Z_w(\mathbf{x})$ is weakly consistent under the assumption that there exists a sequence ω_N with $\omega_N \rightarrow 0$ and $\omega_N N\tau_N^2 \rightarrow \infty$ such that

$$(7) \quad N e^{-\omega_N N\tau_N^2} < m_{\mathbf{x}}, n_{\mathbf{x}} < N(1 - e^{-\omega_N N\tau_N^2}),$$

where $m_{\mathbf{x}}, n_{\mathbf{x}}$ are the corresponding group sizes of $\arg \min_{\mathbf{x}} Z_w(\mathbf{x})$.

THEOREM 2.6 (Strong Consistency). *Under the SBM,*

- If $\frac{N\gamma_N^2}{\log(N)} \rightarrow \infty$, then $\hat{\mathbf{c}} = \arg \max_{\mathbf{x}} Z_d(\mathbf{x})$ is strongly consistent.
- If $\frac{N\tau_N^2}{\log(N)} \rightarrow \infty$ and $P_{11} + P_{22} - P_{12} - P_{21} > 0$, then $\hat{\mathbf{c}} = \arg \max_{\mathbf{x}} Z_w(\mathbf{x})$ is strongly consistent.

- If $\frac{N\tau_N^2}{\log(N)} \rightarrow \infty$ and $P_{11} + P_{22} - P_{12} - P_{21} < 0$, then $\hat{\mathbf{c}} = \arg \min_{\mathbf{x}} Z_w(\mathbf{x})$ is strongly consistent.

REMARK 2.7. In [Amini et al. \(2013\)](#), they consider the SSBM with $P_{11} = P_{22}$ and $P_{12} = P_{21}$. They obtain the weak consistency condition $N\tilde{\tau}^2 = N\frac{(P_{11}-P_{12})^2}{P_{11}+P_{12}} \rightarrow \infty$, which is equivalent with the weak consistency condition we derived here because $\frac{1}{2}\tau^2 < \tilde{\tau}^2 < \tau^2$ in this case.

The proof of [Theorem 2.5](#) and [Theorem 2.6](#) follow the spirit in [Zhao, Levina and Zhu \(2012\)](#) and are provided in [Section 7](#). For the strong consistency, we don't have any additional assumptions except for γ_N, τ_N, N . This can be seen by choosing $\alpha_N = \frac{\log(N)}{N\gamma_N^2}, \beta_N = \frac{\log(N)}{N\tau_N^2}$.

3. Performance exploration. In this section, we explore the performance of Z_w and Z_d on a variety of synthetic datasets, including assortative mixing, disassortative mixing, core-periphery structure, directed graphs, undirected graphs, balanced communities, unbalanced communities, dense graphs and sparse graphs.

We use a greedy method for dividing networks in two by Z_w^{max} (or Z_w^{min}, Z_d): Start from a guess of \mathbf{x} (could be randomly generated), we find among all single changes to \mathbf{x} that is defined as changing one element in \mathbf{x} from s to $1 - s$, and choose the change that will give the biggest increase (or decrease if using Z_w^{min}) in the corresponding Z_w (or Z_d). We make such moves repeatedly until there is no increase (or decrease if using Z_w^{min}) available. We pick many random initial guesses of \mathbf{x} and pick the result with maximum (or minimum if using Z_w^{min}) Z_w (or Z_d). Running many initial guesses sometimes can be time consuming when the number of vertices are pretty large. We suggest using the label assignment from CPL ([Amini et al., 2013](#)) as the initial guess to speed up the algorithm. In this section, we test the performance of $Z_w^{max}, Z_w^{min}, Z_d$ separately. We will discuss the method to automatically choose among these three statistics in [Section 4](#).

We provide experiment results on synthetic data generated from DCSBM, which contains much more flexibility than SBM. We specify the degree heterogeneity parameter θ_i to follow the pareto distribution in this section. We also try other distributions for θ_i and the results are in [Supplementary Material \(Lin and Chen, 2023\)](#). For each node $i \in [n]$, θ_i is sampled independently from a Pareto(α, β) distribution with the density function $f(x | \alpha, \beta) = \frac{\alpha\beta^\alpha}{x^{\alpha+1}} \mathbf{1}_{\{x \geq \beta\}}$, where α and β are called shape and scale parameters, respectively. The shape and scale parameters are adjusted so that the expectation of each θ_i is fixed at 1 to satisfy the identifiability constraint. Given the degree heterogeneity parameters $\{\theta_i\}$ and the connectivity matrix \mathbf{P} , a graph is generated from DCSBM, with the edge probability points from node $i \in C_a$ to node $j \in C_b$ being $\min(1, \theta_i\theta_j P_{ab})$. Note that when all the $\theta_i = 1$, the model becomes the standard SBM.

For comparison, we also apply several algorithms which are reported to have state-of-the-art empirical performance on DCSBM in the existing literature. Note that these methods represent three different categories of community detection methods named modularity-based methods, spectral clustering methods, and likelihood-based methods. Other methods in the same category are likely to have similar performance, hence these methods are representative for comparing our framework with the state-of-the-art literature:

1. Convexified Modularity Maximization (CMM) algorithm in [Chen, Li and Xu \(2018\)](#) is based on convexification of the modularity maximization formulation and a doubly-weighted l_1 norm k-modoids clustering procedure.
2. Modularity Minimization (MMin) in [Newman \(2006b\)](#) is a modularity minimization algorithm, targets at finding disassortative communities.

3. The regularized spectral clustering (Spectral) in [Qin and Rohe \(2013\)](#).
4. The conditional pseudo-likelihood (CPL) maximization algorithm in [Amini et al. \(2013\)](#) maximizes the conditional pseudo-likelihood via EM algorithm, starting with an initial partition provided by regularized spectral clustering.

The synthetic experiments were performed with different connectivity matrix \mathbf{P} 's, representing assortative mixing, disassortative mixing and core-periphery structure. We consider both directed graphs and undirected graphs, balanced design and unbalanced design, dense and sparse graphs in our simulation studies. Note that as the shape parameter of the pareto distribution α increases, the degree parameters $\{\theta_i\}$ become less heterogeneous, hence the DCsBM becomes closer to the standard SBM.

Based on Theorem 2.3, 2.5, 2.6, we can now test the performances of Z_w^{max} , Z_w^{min} , Z_d separately by generating corresponding assortative mixing, disassortative mixing and core-periphery structure. Notice that Z_w and Z_d are not mutually exclusive, which means there are plenty of cases where they are both suitable for discovering the underlying communities, theoretically. Nevertheless, according to practical performance, the statistic Z_w is usually preferred when the mixing type is assortative mixing or disassortative mixing, and Z_d is useful for the core-periphery structure.

Figures 2, 3, 4 show that the misclassification rate of Z_w^{max} , Z_w^{min} , Z_d all decrease as the degree parameters $\{\theta_i\}$ become less heterogeneous (larger value of the shape parameter). In all plots, each point represents the average of 50 independent runs. First, in the assortative mixing graph case, as indicated in Figure 2, Z_w^{max} achieves the highest power for both undirected and directed graphs. CMM, a modularity based method, which is designed for undirected graphs, also has good performance under directed graphs. Spectral methods and CPL are able to be aligned with Z_w^{max} and CMM methods for undirected case, but will have a certain gap with the other two methods when applied to directed graphs. MMin method is not suitable for assortative mixing case, hence being the worst here.

For the disassortative mixing pattern, Figure 3 shows that Z_w^{min} has slightly better accuracy than CPL and Spectral method for undirected case. MMin performs slightly better than Z_w^{min} in the undirected case and they are almost identical in the directed case. CMM completely loses its power for both undirected and directed graphs for the case of disassortative mixing. This is not surprising because CMM is essentially a modularity maximization algorithm. MMin and Z_w^{min} outperform all other methods for directed graphs. Generally speaking, MMin, Z_w^{min} , Spectral and CPL all have satisfying performance for disassortative mixing case, while MMin and Z_w^{min} are preferred for directed graphs.

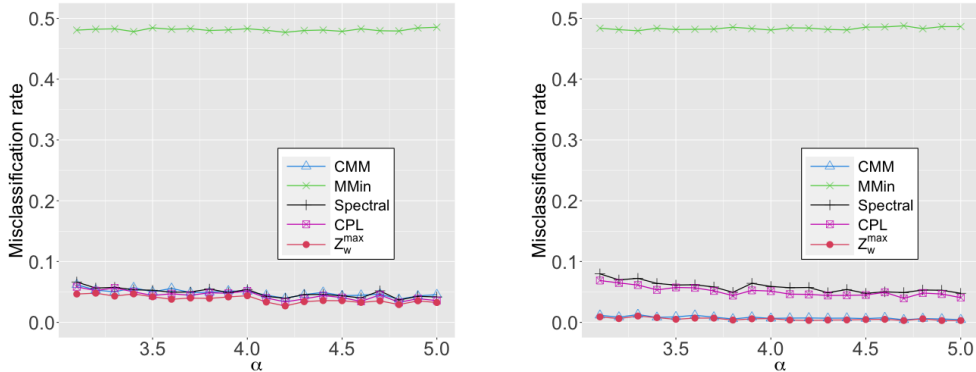


FIG 2. Misclassification rate versus shape parameter of pareto θ for $N = 100$ and 2 equal-sized communities. $\mathbf{P} = [0.5, 0.3; 0.3, 0.5]$. Left panel: undirected graph. Right panel: directed graph.

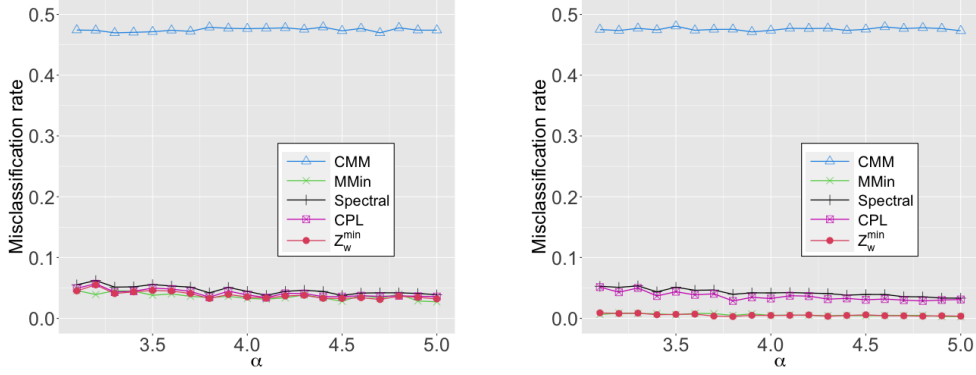


FIG 3. Misclassification rate versus shape parameter of pareto θ for $N = 100$ and 2 equal-sized communities. $\mathbf{P} = [0.3, 0.5; 0.5, 0.3]$. Left panel: undirected graph. Right panel: directed graph.

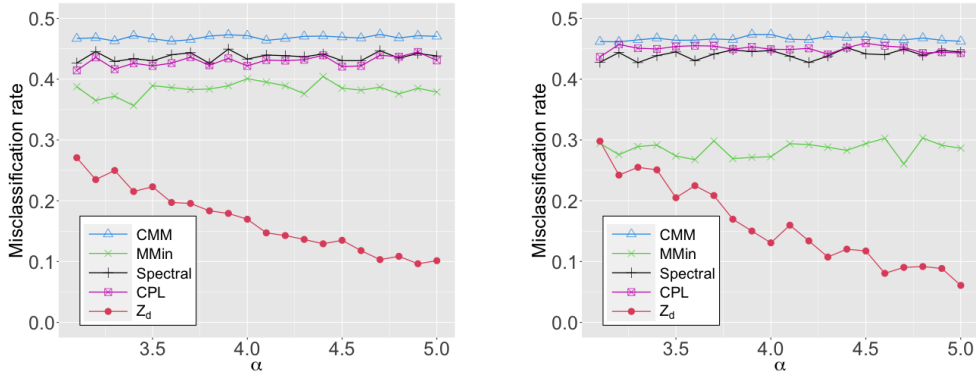


FIG 4. Misclassification rate versus shape parameter of the pareto distribution for $N = 100$ and 2 equal-sized communities. $\mathbf{P} = [0.5, 0.3; 0.3, 0.1]$. Left panel: undirected graph. Right panel: directed graph.

In the case of the core-periphery structure, all other methods lose power hence there is a significant power gap between Z_d and all other methods. The misclassification rate for CMM, CPL and Spectral methods for both undirected and directed graphs are near 50%, which means they are not much better than random guess. The reason behind the failure of these methods are that the periphery part are loosely connected inside them, hence these methods don't recognize that the periphery is a valid community. MMin has a misclassification rate near 40% in the undirected case and 30% in the directed case. That means the model change as the increase of the shape parameter α doesn't affect the dividing mechanism of MMin itself here.

We have similar observations when community sizes are unbalanced, as shown in Figure 5. The sizes of the two communities are 30 and 70, respectively. The left panel stands for the assortative mixing case and the right panel is the core-periphery structure with the small densely inter-connected core. For the assortative mixing in the left panel, all methods are able to achieve high accuracy except for MMin, but Z_w^{max} always achieves the highest power in this setting. For the core-periphery case, only Z_d can reveal the underlying community structure as expected.

The performance of community detection algorithms can be affected by the density of the graph. The previous examples are all about relatively dense graphs. Here we also consider less dense graphs. In Figure 6, the left panel is an assortative mixing case with the connectivity matrix being $\mathbf{P} = [0.1, 0.05; 0.05, 0.1]$ and the community sizes being

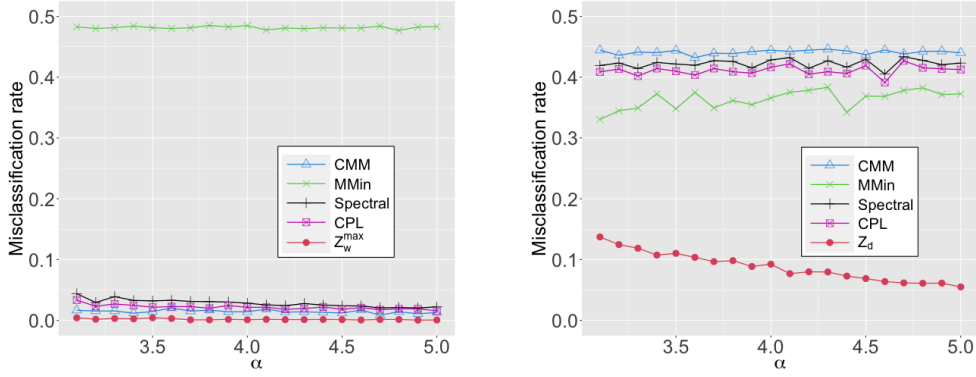


FIG 5. Misclassification rate versus shape parameter of pareto θ with $m = 30$ and $n = 70$. Left panel: $\mathbf{P} = [0.5, 0.25; 0.25, 0.5]$, directed graph. Right panel: $\mathbf{P} = [0.5, 0.3; 0.3, 0.1]$, undirected graph.

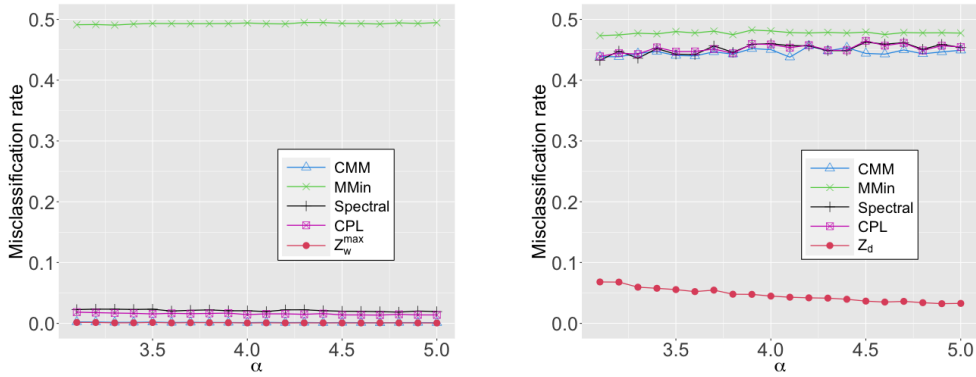


FIG 6. Misclassification rate versus shape parameter of pareto θ . Left panel: $\mathbf{P} = [0.1, 0.05; 0.05, 0.1]$, $m = 300$, $n = 300$, directed graph. Right panel: $\mathbf{P} = [0.1, 0.03; 0.03, 0.01]$, $m = 100$, $n = 500$, undirected graph.

$m = n = 300$. The right panel is a core-periphery structure with the connectivity matrix $\mathbf{P} = [0.1, 0.03; 0.03, 0.01]$ and the community sizes being $m = 100$, $n = 500$. In Figure 6, left panel shows that CMM has similar power with Z_w^{max} . CPL and Spectral again suffer from the directed graph performance gap in sparse case. While for the core-periphery structure in the right panel, things remain unchanged. The statistic Z_d is still the only one that can achieve stable high power. All the other methods are as poor as random guess.

4. UBSea community detection framework. All the simulation results in Section 3 provide strong evidence that Z_w^{max} , Z_w^{min} , Z_d are powerful when the underlying generation scheme of the true data lies within their consistency regions. From Theorem 2.3, 2.5, 2.6, it is reasonable to say that, when $N\gamma_N^2 \rightarrow \infty$, we should use Z_d as the community detection criterion; when $N\tau_N^2 \rightarrow \infty$ we should use Z_w^{max} or Z_w^{min} as the criterion depend on the sign of $P_{11} + P_{22} - P_{12} - P_{21}$. The question remains, how to choose among Z_w^{max} , Z_w^{min} , Z_d if there is no prior information on the connectivity matrix available to us. Here we discuss two possible solutions to automatically choose among these three statistics, γ - τ criterion in Section 4.1, penalized likelihood criterion in Section 4.2, and check their performance in Section 4.3.

4.1. γ - τ criterion. Based on Theorem 2.5, when Z_d should be used, it is expected to have a large value of γ^2 when we have moderate to large sample size; when Z_w should be used, it is expected to have a large value of τ^2 . Thus, we first fit the network using Z_d , Z_w^{\max} and Z_w^{\min} separately and then calculate corresponding $\hat{\gamma}^2$ and $\hat{\tau}_{\max}^2, \hat{\tau}_{\min}^2$ values, pick the largest one as the proper statistic. We will see that this criterion, based on the consistency theory on the stochastic block model, is well-behaved when the true underlying model is exactly SBM, and to a certain extent for the DCSBM.

4.2. Penalized likelihood criterion. Likelihood method is arguable consistent under DCSBM when θ_i 's are discrete (Zhao, Levina and Zhu, 2012). However, we notice that, for the finite sample with continuous θ_i 's case, there is always a cost associated with fitting the extra complexity of the degree-corrected model. To be more specific, if we view the heterogeneity of θ_i 's as part of the model complexity under corrected model, the statistic Z_w and Z_d always try to fit a more complex model when it is not suitable for the true underlying connectivity matrix as we discussed before. Thus, inspired by the penalized likelihood raised in Wang and Bickel (2017) for estimating the number of communities using penalized likelihood, we propose the following criterion to choose between Z_w and Z_d :

$$(8) \quad \begin{aligned} L(\mathbf{A}; \mathbf{x} | \mathbf{P}) = & \sum_{i=1}^N \sum_{j=1}^N (A_{ij} \log(P_{c_i(\mathbf{x})c_j(\mathbf{x})} \theta_i \theta_j) + (1 - A_{ij}) \log(1 - P_{c_i(\mathbf{x})c_j(\mathbf{x})} \theta_i \theta_j)) \\ & - \lambda (\text{Var}(\theta_{c_1}(\mathbf{x})) + \text{Var}(\theta_{c_2}(\mathbf{x}))) \sum_{i,j} A_{ij}, \end{aligned}$$

where λ is a tuning parameter, $c_i(\mathbf{x}) = 1$ if $\mathbf{x}_i = 1$ and $c_i(\mathbf{x}) = 2$ if $\mathbf{x}_i = 0$, $\theta_{c_1}(\mathbf{x})$ and $\theta_{c_2}(\mathbf{x})$ represent the node parameters for community 1 and community 2 determined by the label assignment \mathbf{x} , with a slight abuse of notation. Criterion (8) is typically defined for directed graphs. For undirected graphs, we use the same criterion with the natural undirected graph constraint $j \leq i$ in the sums.

When in use, we found that Z_d tends to fit highly biased communities assignments when it is not the correct criterion, resulting in unexpected large value of the penalty term. To avoid the penalty term dominating the penalized likelihood value fluctuation, and make the criterion more stable, we replace the penalty term for Z_d to be:

$$\max \left(\text{Var}(\theta_{c_1}(\mathbf{x})) \left(\sum_{c_i=c_j=1} A_{ij} \right), \text{Var}(\theta_{c_2}(\mathbf{x})) \left(\sum_{c_i=c_j=2} A_{ij} \right) \right).$$

Our current choice for the tuning parameter λ is 0.12 for both directed and undirected graphs. Further investigation may be performed to analyze the choice of the tuning parameter λ .

To have an analytical expression for the MLE of θ_i 's, we follow the trick in Karrer and Newman (2011), use a poisson approximation instead of the original binomial distribution for A_{ij} . As a result, the MLE of θ_i under undirected graph is

$$(9) \quad \hat{\theta}_i = \frac{k_i}{\kappa_{c_i}},$$

where k_i is the degree of node i , κ_r is the average degree in group r . Similarly, the MLE of θ_i for directed graph has the following form:

$$(10) \quad \hat{\theta}_i = \frac{k_i^{in} + k_i^{out}}{\kappa_{c_i}^{in} + \kappa_{c_i}^{out}},$$

where k_i^{in} is the in degree of node i and k_i^{out} is the out degree of node i , κ_r^{in} is the average in degree of nodes in group r and κ_r^{out} is the average out degree of nodes in group r .

It is worth pointing out that for a long time period, people tend to develop the modularity-based community detection framework assuming the prior knowledge that the mixing pattern is actually assortative mixing. In essence, this implies that they prioritize maximizing modularity to identify communities, assuming that the mixing pattern is primarily assortative and test their algorithms on assortative mixing dataset. However, researchers from different domains frequently apply modularity to disassortative or core-periphery communities and feel confused about the poor results. Therefore, it is needed to develop a framework that spends more effort discussing the different mixing types instead of simply fit a pre-determined community structure, which can benefit people from different domains with various research needs.

By adopting the γ - τ criterion or penalized likelihood criterion, we bring in the new insight on network community structure: There are different possible community structures (assortative mixing, disassortative mixing and core-periphery structure) for a given network simultaneously, but some are more significant. Our task in community detection is actually first extract all the possible community structures in the current category of mixing patterns. After that, we analyze among these possible patterns, which one is more significant under some scientific rules, for instance, the γ - τ and penalized likelihood criterion in our UBSea framework.

4.3. Performance of γ - τ criterion and penalized likelihood criterion. It is relatively easier to decide whether to use Z_w^{\max} , Z_w^{\min} or Z_d under the Stochastic Block Model comparing to its generalization Degree Corrected Stochastic Block Model.

Figure 7 displays the corresponding values of $N\gamma^2$, $N\tau_{\min}^2$ and $N\tau_{\max}^2$ for different mixing types under standard SBM. From left to right, the underlying true mixing types are assortative mixing, disassortative mixing and core-periphery, respectively. We can see that the γ - τ criterion is pretty stable and perfect under different settings for the SBM since the values of the suitable mixing type is always the highest and much larger than the other two. For example, when the connectivity matrix $\mathbf{P} = [0.5, 0.3; 0.3, 0.5]$ in the left most panel, the value of $N\tau_{\max}^2$ is significantly larger than the value of $N\tau_{\min}^2$ and $N\gamma^2$. Similar results were seen in the other two panels.

However, for the more flexible DCSBM, γ - τ criterion often loses power. To assess the performance of the γ - τ criterion under the DCSBM, we test under different connectivity matrices: (I): $\mathbf{P} = \begin{bmatrix} 0.1 & 0.02 \\ 0.02 & 0.1 \end{bmatrix}$, (II): $\mathbf{P} = \begin{bmatrix} 0.3 & 0.5 \\ 0.5 & 0.3 \end{bmatrix}$, (III): $\mathbf{P} = \begin{bmatrix} 0.5 & 0.2 \\ 0.2 & 0.5 \end{bmatrix}$, (IV): $\mathbf{P} = \begin{bmatrix} 0.5 & 0.3 \\ 0.3 & 0.5 \end{bmatrix}$, (V): $\mathbf{P} = \begin{bmatrix} 0.6 & 0.3 \\ 0.3 & 0.1 \end{bmatrix}$. Suppose the misclassification rate for Z_d , Z_w^{\min} and Z_w^{\max} are ϵ_d , ϵ_w^{\min} and ϵ_w^{\max} , respectively. Also, denote ϵ to be the misclustering rate of γ - τ criterion or penalized likelihood criterion. The success rate of the criterion out of s independent runs is defined

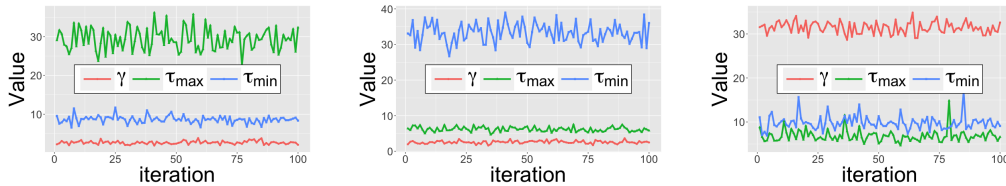


FIG 7. $N\gamma^2$, $N\tau_{\max}^2$ and $N\tau_{\min}^2$ for $N = 100$ and 2 equal-sized clusters generated from SBM model as directed graphs. From left to right: $\mathbf{P} = [0.5, 0.3; 0.3, 0.5]$, $\mathbf{P} = [0.3, 0.5; 0.5, 0.3]$, $\mathbf{P} = [0.5, 0.3; 0.3, 0.1]$

as:

$$S = \frac{1}{s} \sum_{i=1}^s \mathbb{I}(\epsilon \leq (1 + \psi) \min\{\epsilon_d, \epsilon_w^{\min}, \epsilon_w^{\max}\}).$$

The tolerance rate ψ is chosen to be 0.1 in the simulations below for both γ - τ criterion and penalized likelihood criterion.

Figure 8 show that Setting IV (assortative mixing) and Setting II (disassortative mixing) are with the lowest success rate for both directed and undirected graphs, whereas Setting V (core-periphery) have relatively high success rate. Setting III is doing well because it has stronger assortative structure comparing to Setting IV. That indicates the γ - τ criterion is too aggressive in a sense that it has a preference for core-periphery structure rather than the assortative mixing pattern or disassortative mixing pattern. We want our framework, on the contrary, to have a preference for assortative mixing and disassortative mixing, and only leans toward core-periphery structure when the evidence is much more convincing. In another word, we want our framework to be more conservative for determining a core-periphery structure. We found that penalized likelihood criterion would offer better and satisfying power under DCSBM, hence also desired under SBM if computationally fast. As a consequence, Penalized Likelihood Criterion is our main criterion for choosing between Z_w and Z_d .

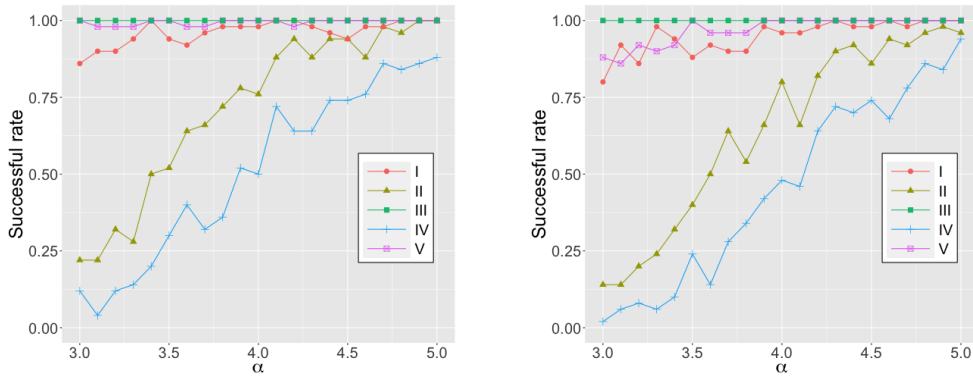


FIG 8. Success rate of the γ - τ criterion, tolerance rate $\psi = 0.1$ for different settings of the connectivity matrix. The community sizes are 50 each. Left panel: undirected graphs. Right panel: directed graphs.

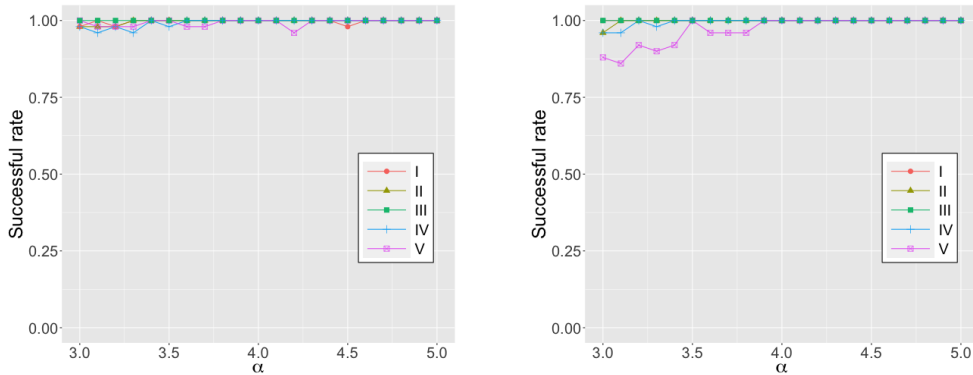


FIG 9. Success rate of the penalized likelihood criterion with tuning parameter $\lambda = 0.12$ and tolerance rate $\psi = 0.1$ for different settings of the connectivity matrix. The community sizes are 50 each. Left panel: undirected graphs. Right panel: directed graphs.

Figure 9 show that no matter for undirected graphs or directed graphs, the success rate of penalized likelihood criterion is nearly 100% for undirected graphs and exceeds 80% for directed graphs. As a comparison, the γ - τ criterion attained only a power near 20% for Setting (II) and Setting (IV) in Figure 8 in the beginning of the same parameter settings. The largest value of θ when $\alpha = 3$ is often larger than 4, which means the degree heterogeneity inside every block is still considerable. Hence, the Penalized Likelihood criterion can have high power for a wide range of networks generated from DCSBM.

Figure 10, 11, 12 directly show the results of our UBSea method applied to the assortative setting, disassortative setting and core-periphery for undirected graphs and directed graphs using the penalized likelihood criterion. Comparing to Figure 2, 3, 4, the misclassification rate increased a little bit in the beginning but not much.

From now on, our default procedure for UBSea community detection will be as follows: we first fit the networks with $Z_d, Z_w^{max}, Z_w^{min}$, respectively, and then choose among the three community detection results using the penalized likelihood criterion.

5. Real Data Analysis.

5.1. *US politics book and UK faculty network data sets.* In this section, we investigate the performance of our UBSea framework on two traditional benchmarks:

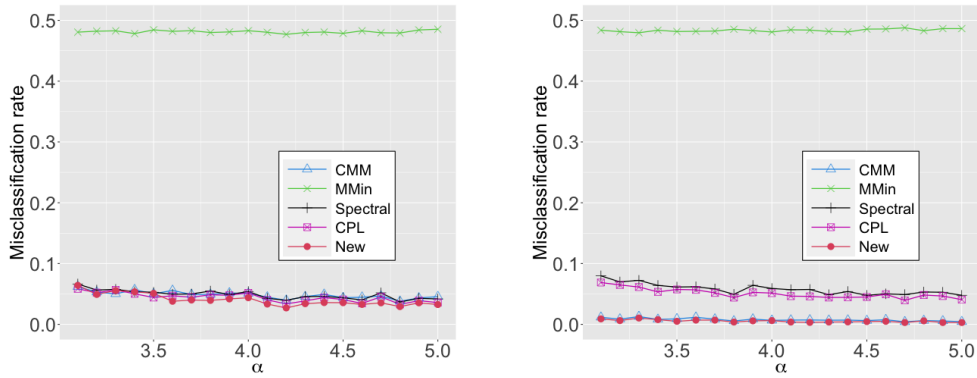


FIG 10. Misclassification rate versus shape parameter of pareto θ for $N = 100$ and 2 equal-sized clusters. $\mathbf{P} = [0.5, 0.3; 0.3, 0.5]$. Left panel: undirected graph. Right panel: directed graph.

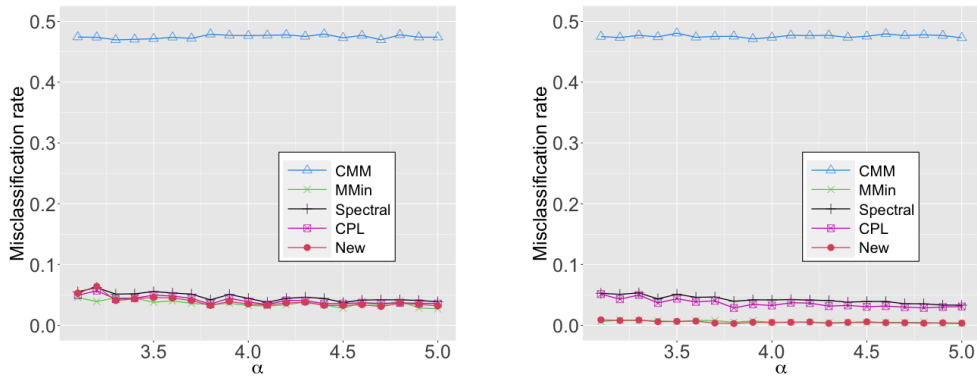


FIG 11. Misclassification rate versus shape parameter of pareto θ for $N = 100$ and 2 equal-sized clusters. $\mathbf{P} = [0.3, 0.5; 0.5, 0.3]$. Left panel: undirected graph. Right panel: directed graph.

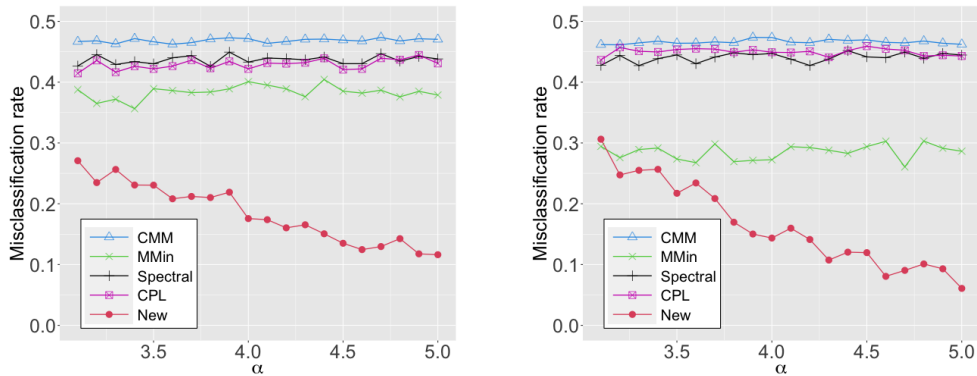


FIG 12. Misclassification rate versus shape parameter of pareto θ for $N = 100$ and 2 equal-sized clusters. $\mathbf{P} = [0.5, 0.3; 0.3, 0.1]$. Left panel: undirected graph. Right panel: directed graph.

- the US politics book network
- the UK faculty network

The US politics book network data was first compiled by Valdis Krebs and is unpublished. The data set can be found on Krebs’s website. Nodes represent books sold on Amazon.com about US politics. Edges represent frequent co-purchasing of books by the same buyer. Nodes have been given values ‘l’, ‘n’ or ‘c’ to indicate whether they are ‘liberal’, ‘neutral’ or ‘conservative’. These alignments were assigned separately by Mark Newman, we take that as the ground truth in this data set. Here we focus on the ‘liberal’ and ‘conservative’ books, resulting in a total number of 92 nodes and 374 undirected edges. The UK faculty network in [Nepusz et al. \(2008\)](#) contains a network in a given UK university of four separate schools. The nodes represent members of the academic staff. An edge between two members represents that they are friends, according to a questionnaire. There are 33 nodes from school ‘1’, 27 nodes from school ‘2’, 19 nodes from school ‘3’ and 2 nodes from school ‘4’. We focus on the first three schools and analyze all the three combinations between two schools. For example, the sub-graph formed by the staffs from school ‘1’ and school ‘2’ will be analyzed as UKfaculty12 in Table 1.

TABLE 1
Error rates on the Polbooks and UKfaculty data sets.

Methods	Polbooks	UKfaculty12	UKfaculty23	UKfaculty13
New	2/92	1/60	0/46	1/52
CMM	2/92	5/60	6/46	11/52
CPL	2/92	3/60	2/46	2/52
Spectral	3/92	2/60	1/46	1/52
MMin	43/92	28/60	23/46	23/52

From Table 1, we can see that most methods have similar behavior on these traditional benchmarks as expected, while MMin is certainly not suitable for these traditional assortative benchmarks. For the Polbooks data set, UBSea, CMM and CPL all achieve a very low error rate, which is 2 out of 92 nodes. Spectral method performs slightly worse with one more node mis-classified. For the UK faculty data set, CMM seems to be less powerful compared with other methods. UBSea, CPL and Spectral all have high stability and accuracy on this data set.

It is worth pointing out that these benchmarks are known to be assortative mixing beforehand. Hence all the methods target on assortative mixing are expected to perform well on

these benchmarks without going into discussing the mixing type step. Our UBSea framework, however, gave these community detection results based on the Penalized Likelihood criterion. We are doing this because our framework of community detection are based on a different perspective of communities mixing dynamic. We are more convinced that for a given network, assortative mixing, disassortative mixing and core-periphery structure will exist simultaneously. For these political books and UK faculty network analyzed here, the assortative mixing pattern is more significant than core-periphery structure and disassortative mixing structure as the result suggested by our UBSea framework. This is an important perspective because for instance, it is also natural to think the UK faculty network, or the general friendship networks, will exhibit the core-periphery structure with some popular people form the core and others form the periphery. Our UBSea framework confirms that the assortative mixing evidence is much more significant than core-periphery structure on this UK faculty data set indicating by the penalized likelihood criterion.

5.2. *Word Adjacency Network.* This data set was compiled by Newman (2006b) from the novel David Copperfield by Charles Dickens. This network consists of the 60 most commonly occurring nouns and the 60 most commonly occurring adjectives connects any pair of words that appear adjacently in the text, resulting in an undirected graph. Excluding eight words which are disconnected from the rest leaves a network with 112 nodes. We treat ‘noun’ and ‘adjective’ words as two different communities and the goal is to recover these two community labels through the network structure. The data is plotted in Figure 13.

This word-adjacency network follows strong disassortative mixing pattern. It is common that an adjective word will followed by a noun. Table 2 shows UBSea, CPL and MMin

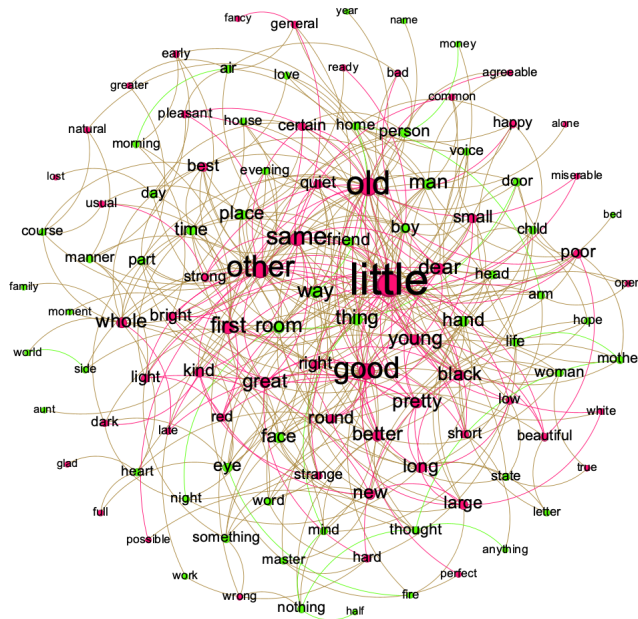


FIG 13. Adjective-Noun network. Red group is adjective words while green group is noun words. Node size is scaled based on node degree.

TABLE 2
Mis-clustering rate on word-adjacency Network

Method	New	CPL	CMM	Spectral	MMin
mis. rate	19/112	18/112	55/112	42/112	20/112

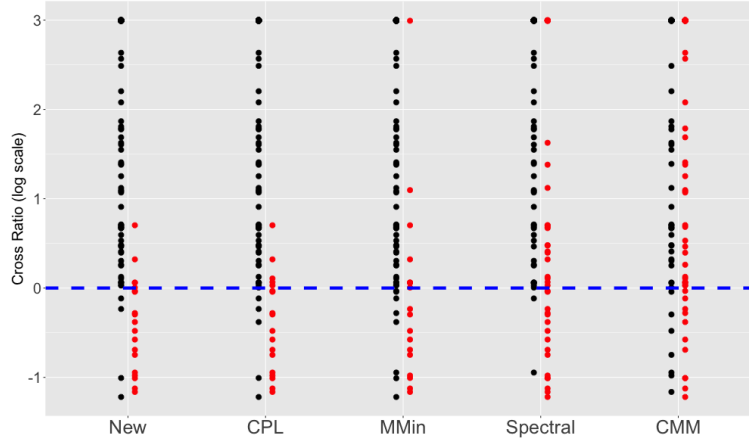


FIG 14. Scatter plots of log-scale cross ratio. Red (Black) color stands for mis-matched (matched) points comparing to the true label. Inf values are truncated to be 3.

methods achieve similar accuracy rate on this data set. Among these words, there are some neutral words can behave like both noun and adjective, for instance, “pretty, black”. To better evaluate the performance of different methods, we here define the log-scale cross ratio of node i under label assignment \mathbf{x} to be $R(i, \mathbf{x}) = \log \frac{b(i)}{w(i)}$, where $b(i)$ represents the number of between edges, that is, edges connect i with vertices from different communities, $w(i)$ is the number of within same group edges. Figure 14 shows the scatter plots of the log-scale cross ratio for different methods using the true label. Since some points don’t have within community edges, i.e., $w(i) = 0$, we manually set those log-scale cross ratio to be 3 only to better visualize the results. The red points stand for the mis-matched points for different methods comparing to the underlying truth. We see that most of the mis-matched points for the New method have the log cross ratio less than 0, meaning that the cross edges are less than the within group edges. In this sense, these words break the disassortative structure of the network. It might be better to group the words into three groups considering these neutral words, which we leave for future work. CMM totally failed to recover the underlying disassortative mixing structure. Spectral method, which achieves slightly better performance than CMM in Table 2, is again much worse than UBSea and CPL. MMin is slightly better but not as good as New and CPL.

5.3. *A co-citation network.* This dataset was provided by Baker (1992), who studied co-citations among social work journals on a sample of 20 social network journals included in the SSCI Guide. His data consisted of the number of citations from one journal to another journal during a 1-year period (1985-1986), here we follow Borgatti and Everett (2000) to dichotomize the data. Therefore, there will only be one directed edge from Journal A to journal B if Journal B was once cited in Journal A. In the end, this network contains 20 nodes and 107 directed edges. We assume the identified core journals in Borgatti and Everett (2000): “SSR”, “CYSR”, “JSWE”, “SCW” and “SW” as the underlying ground truth label for core cluster.

Figure 15 displays the visualization for this co-citation network using community detection result in Borgatti and Everett (2000). Green edges are connections in the core, red edges are edges within the periphery and grey ones the cross edges. We see that there are very few edges (red edges) within the periphery except for one journal (“CW”) in the middle of the picture. In fact, our method puts this journal in the core instead of “CYSR” journal in

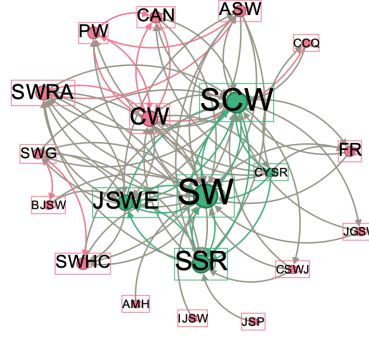


FIG 15. Visualization of co-citation network using community detection results by “ground truth”. Red nodes stand for the periphery and green for the core. Red edges stand for the edges inside the periphery, green edges stand for the edges inside the core and the grey ones stand for cross edges. Node size is scaled using in-degree.

TABLE 3

Mis-clustering rate on co-citation Network for different algorithms. mis.rate represents the overall misclustering rate. mis.core stands for the misclustering rate for the core.

Method	New	CPL	CMM	Spectral	MMin
mis.rate	2/20	8/20	5/20	9/20	3/20
mis.core	1/5	4/5	2/5	4/5	2/5

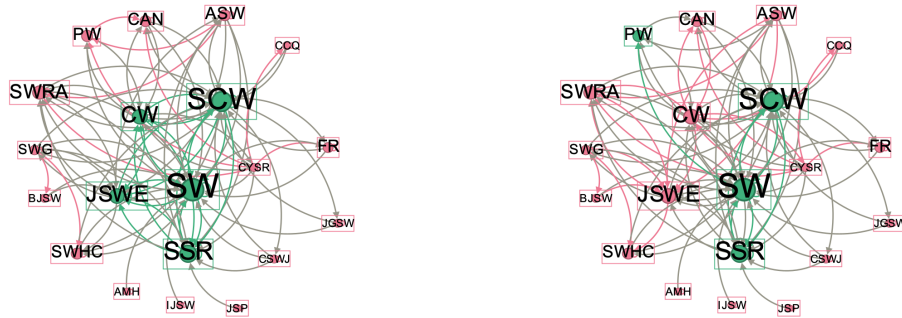


FIG 16. Visualization of co-citation network using UBSea method (left) and MMin method (right).

the middle right of the picture. Table 3 displays the misclustering rate for different methods. Here, mis.rate stands for the overall misclustering rate and mis.core shows the unidentified nodes for the core found by Borgatti and Everett (2000). We see UBSea method has the lowest overall misclustering rate and can identify the most number of core nodes. CPL and Spectral produce poor results. MMin method has fair result here. To compare the results by UBSea and MMin, Figure 16 show that UBSea result is clearly better because MMin puts “PW” in the core and rules out both “CW” and “JSWE”. It also seems more reasonable to put “CW” in the core by comparing Figure 15 and Figure 16. Figure 17 show the adjacency plots of “ground truth” and UBSea result with core in the bottom left. We see the adjacency matrix in the right panel (UBSea) has a more densely connected core. Further investigation shows that Borgatti and Everett (2000) converts the graph to undirected for their algorithm.

6. Conclusion and Discussion. In this paper, we studied the problem of community detection for network data with two underlying communities. We extended modularity in a strategic way and proposed a novel UBSea community detection framework. This new framework is able to detect three different kinds of mixing types: assortative mixing, disassortative

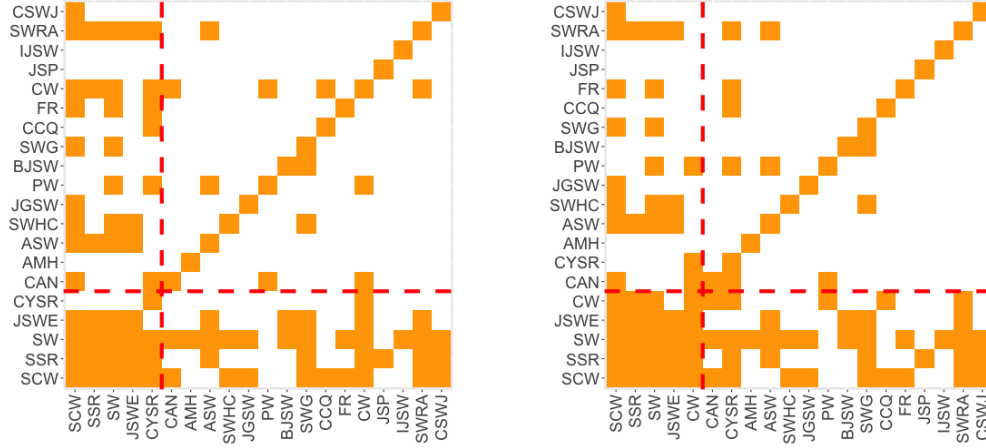


FIG 17. Left panel: adjacency plot of the community detection result in [Borgatti and Everett \(2000\)](#) for co-citation network.. Right panel: adjacency plot of UBSea method for co-citation network. Orange color block represents a directed edge from row journal to column journal.

mixing and core-periphery structure simultaneously. It can be applied to both directed networks and undirected networks without any generalization or extra data pre-processing steps. We provided both weak consistency and strong consistency results with similar SNR condition in the literature of SBM for the case of two communities.

After we successfully use the UBSea framework to deal with the problem of two communities. The next step is how to extend the framework to more than two communities. We develop this framework under the simple SBM with two communities. While simulation results show that this framework also enjoys extremely good performance for data generated from the Degree-Corrected Stochastic Block Model under a wide range of settings, which can be approximated by the stochastic block model with multiple communities, making it promising to generalize this framework to SBM with multiple communities, typically for data generated from Binary Tree Stochastic Block Model ([Li et al., 2022](#)). We leave the task of multiple communities detection under BTSBM as part of our future work.

As a concluding remark, we want to discuss the expectation used in modularity. We here explain the reason why we want to adopt a different $\mathbb{E}A_{ij}$, or the null model in Section 2.1. In fact, we also tried to use a modified criterion Q_d based on modularity without changing $\mathbb{E}A_{ij}$, in a hope to deal with the core-periphery structure directly. Unfortunately, it does not lead to desired properties as Z_d has. Reasons and experiments are demonstrated in Appendix A. Briefly speaking, in the history of community detection, the minimum cut algorithm is an early attempt by just minimizing the cross community edges, or maximizing the edges within the communities. Modularity improves this idea by subtracting the expectation, or $\mathbb{E}A_{ij}$ within the communities. The expectation was calculated under an approximate configuration model so that the degree distribution under the null model is similar to the data. In another word, the degree distribution of the data becomes an additional tool in the spirit of modularity. As we pointed out earlier, in the core-periphery case, the degree deviation measurement inside the core is positive and the deviation measurement inside the periphery is negative, hence cancelled out when added together. Thus the degree is not a useful tool in core-periphery case. Here in this paper, we adopt a much simpler null model without considering the degree distribution, but we see better performance in almost all synthetic settings and real data applications. Together with the failure of extending modularity without changing $\mathbb{E}A_{ij}$, it now answers the motivation for us to adopt a different $\mathbb{E}A_{ij}$.

7. Proofs for weak and strong consistency. In this section, we prove the consistency results for Z_d and Z_w in Theorem 2.5 and Theorem 2.6.

PROOF. We first analyze Z_d under directed graphs. Notice that

$$\begin{aligned}
Z_d^P(\mathbf{x}) &= \frac{R_d^P(\mathbf{x}) - \mu_d^P(\mathbf{x})}{\sigma_d(\mathbf{x})} \\
&= \frac{R_d^P(\mathbf{x}) - \mu_d^P(\mathbf{x})}{\sqrt{(m - \Delta_1 + \Delta_2)(n + \Delta_1 - \Delta_2)}} \sqrt{\frac{N(N-1)}{|G| + q_1 + |G|^2 \frac{N-4}{N} - q_2}} \\
&= \tilde{Z}_d^P(\mathbf{x}) \sqrt{\frac{N(N-1)}{|G| + q_1 + |G|^2 \frac{N-4}{N} - q_2}}, \\
Z_d(\mathbf{x}) &= \frac{R_d(\mathbf{x}) - \mu_d(\mathbf{x})}{\sigma_d(\mathbf{x})} \\
&= \frac{R_d(\mathbf{x}) - \mu_d(\mathbf{x})}{\sqrt{(m - \Delta_1 + \Delta_2)(n + \Delta_1 - \Delta_2)}} \sqrt{\frac{N(N-1)}{|G| + q_1 + |G|^2 \frac{N-4}{N} - q_2}} \\
&= \tilde{Z}_d(\mathbf{x}) \sqrt{\frac{N(N-1)}{|G| + q_1 + |G|^2 \frac{N-4}{N} - q_2}},
\end{aligned}$$

where m, n are the true block sizes, $\tilde{Z}_d^P(\mathbf{x}) = \frac{R_d^P(\mathbf{x}) - \mu_d^P(\mathbf{x})}{\sqrt{(m - \Delta_1 + \Delta_2)(n + \Delta_1 - \Delta_2)}}$ and $\tilde{Z}_d(\mathbf{x}) = \frac{R_d(\mathbf{x}) - \mu_d(\mathbf{x})}{\sqrt{(m - \Delta_1 + \Delta_2)(n + \Delta_1 - \Delta_2)}}$. Since $\sqrt{\frac{N(N-1)}{|G| + q_1 + |G|^2 \frac{N-4}{N} - q_2}}$ does not depend on \mathbf{x} , we can only consider \tilde{Z}_d and \tilde{Z}_d^P in the following context.

LEMMA 7.1. *If Y_1, \dots, Y_I are independent, $|Y_i| \leq 1, \mathbb{E}Y_i = 0, S_I = \sum_{i=1}^I Y_i$, then*

$$P(|S_I| \geq \omega) \leq 2 \exp\left(-\frac{\omega^2/2}{\text{Var}(S_I) + \omega/3}\right) \leq 2 \exp\left(-\min\left(\frac{\omega^2}{3\text{Var}(S_I)}, \frac{\omega}{2}\right)\right).$$

Lemma 7.1 is a special version of the well-known Bernstein concentration inequality. Now, suppose there are two communities, with community sizes m and n , $N = m + n$ and the proportions $\pi_1 = \frac{m}{N}, \pi_2 = \frac{n}{N}$. We prove the consistency results via three steps. Details to obtain (11), (12), (13) are provided in Supplementary Material (Lin and Chen, 2023).

Step I: Let ϵ_N be in the range

$$\frac{\max(P)}{N} \ll \epsilon_N^2 \ll (2\pi_1 P_{11} - 2\pi_2 P_{22} - (\pi_1 - \pi_2)(P_{12} + P_{21}))^2.$$

Notice that ϵ_N is well defined because the ratio between the right hand side and left hand side is $N\gamma_N^2 \rightarrow \infty$. We prove that:

$$(11) \quad P\left(\max_{\mathbf{x}} \frac{1}{N} |\tilde{Z}_d(\mathbf{x}) - \tilde{Z}_d^P(\mathbf{x})| \geq \epsilon_N\right) \rightarrow 0.$$

On one hand, if we have $\frac{N\gamma_N^2}{\log(N)} \rightarrow \infty$, we can achieve (11) without any assumption. On the other hand, when we only have $N\gamma_N^2 \rightarrow \infty$, we rule out the deviance in boundaries by

assumption (5) to achieve (11).

Step II: we prove that there exists $\delta_N \rightarrow 0$ such that, when $\|\mathbf{x} - \mathbf{x}^*\| \geq \delta_N$, we have:

$$(12) \quad \frac{1}{N}(\tilde{Z}_d^P(\mathbf{x}^*) - \tilde{Z}_d^P(\mathbf{x})) > 2\epsilon_N,$$

where $\|\mathbf{x} - \mathbf{x}^*\|$ is defined to be $\min\left(\frac{\Delta_1}{m} + \frac{\Delta_2}{n}, 2 - \frac{\Delta_1}{m} - \frac{\Delta_2}{n}\right)$. For convenience, assume $\frac{\Delta_1}{m} + \frac{\Delta_2}{n} \leq 1$. Otherwise we can do labels permutation. Therefore, $\|\mathbf{x} - \mathbf{x}^*\| = \frac{\Delta_1}{m} + \frac{\Delta_2}{n}$. Furthermore, we show that δ_N essentially should satisfy:

$$(13) \quad \delta_N > \frac{\max(4\pi_1, 4\pi_2)}{\sqrt{\pi_1\pi_2}} \frac{2\epsilon_N}{|2\pi_1P_{11} - 2\pi_2P_{22} - (\pi_1 - \pi_2)(P_{12} + P_{21})|}.$$

By the choice of ϵ_N in Step I, the right hand side goes to 0, thus we enforce $\delta_N \rightarrow 0$.

Step III: Since (12)

$$\begin{aligned} & P\left(\max_{\|\mathbf{x} - \mathbf{x}^*\| > \delta_N} \tilde{Z}_d(\mathbf{x}) < \tilde{Z}_d(\mathbf{x}^*)\right) \\ & \geq P\left(\frac{1}{N} \max_{\|\mathbf{x} - \mathbf{x}^*\| > \delta_N} |\tilde{Z}_d(\mathbf{x}) - \tilde{Z}_d^P(\mathbf{x})| < \epsilon_N, \frac{1}{N} |\tilde{Z}_d(\mathbf{x}^*) - \tilde{Z}_d^P(\mathbf{x}^*)| < \epsilon_N\right) \\ & \rightarrow 1 \quad (\text{By step I and step II}), \end{aligned}$$

We have the weak consistency. **To prove strong consistency**, we need to further analyze the property within the interval $\|\mathbf{x} - \mathbf{x}^*\| \leq \delta_N$. Without confusion, suppose that $\frac{\Delta_1}{m} + \frac{\Delta_2}{n} = \rho_N$ where $\rho_N \leq \delta_N$, δ_N is our specified upper bound in the previous weak consistency section. With

$$\tilde{Z}_d(\mathbf{x}) - \tilde{Z}_d(\mathbf{x}^*) = (\tilde{Z}_d(\mathbf{x}) - \tilde{Z}_d^P(\mathbf{x})) - (\tilde{Z}_d(\mathbf{x}^*) - \tilde{Z}_d^P(\mathbf{x}^*)) - (\tilde{Z}_d^P(\mathbf{x}^*) - \tilde{Z}_d^P(\mathbf{x})).$$

Define $H = |2\pi_1P_{11} - 2\pi_2P_{22} - (\pi_1 - \pi_2)(P_{12} + P_{21})|$. By intermediate result in Step II,

$$\frac{1}{N}(\tilde{Z}_d^P(\mathbf{x}^*) - \tilde{Z}_d^P(\mathbf{x})) > c(\pi_2, \pi_2)H\rho_N,$$

where $c(\pi_1, \pi_2)$ is some constant of π_1, π_2 . By resolving the constants in ρ_N , first we estimate the probability that for $\|\mathbf{x} - \mathbf{x}^*\| = \rho_N$,

$$P\left(\left\{(\tilde{Z}_d(\mathbf{x}) - \tilde{Z}_d^P(\mathbf{x})) - (\tilde{Z}_d(\mathbf{x}^*) - \tilde{Z}_d^P(\mathbf{x}^*))\right\} > NH\rho_N\right).$$

Case 1: if $\Delta_1 = \Delta_2 = \Delta$. Let

$$A_1 = \{(i, j) | \mathbf{x}_i = \mathbf{x}_j = 1\}, A_0 = \{(i, j) | \mathbf{x}_i = \mathbf{x}_j = 0\},$$

$$B_1 = \{(i, j) | \mathbf{x}_i^* = \mathbf{x}_j^* = 1\}, B_0 = \{(i, j) | \mathbf{x}_i^* = \mathbf{x}_j^* = 0\}.$$

Hence

$$\begin{aligned} & (\tilde{Z}_d(\mathbf{x}) - \tilde{Z}_d^P(\mathbf{x})) - (\tilde{Z}_d(\mathbf{x}^*) - \tilde{Z}_d^P(\mathbf{x}^*)) \\ & = \frac{1}{\sqrt{mn}} \left(\sum_{i,j \in (A_1 \setminus B_1) \cup (B_1 \setminus A_1)} (A_{ij} - \mathbb{E}_2(A_{ij})) - \sum_{i,j \in (A_0 \setminus B_0) \cup (B_0 \setminus A_0)} (A_{ij} - \mathbb{E}_2(A_{ij})) \right) = I_0. \end{aligned}$$

By Lemma 7.1 again,

$$P(|I_0| \geq NH\rho_N) \lesssim \exp\left(-\min\left(t_1\sqrt{mn}NH\rho_N, t_2\frac{N^2H^2\rho_N^2mn}{\max(P)(N-\Delta)\Delta}\right)\right),$$

where t_1, t_2 are some constants. Simple calculation verified that when $\|\mathbf{x} - \mathbf{x}^*\| < \delta_N$, where δ_N small, the second term will be the dominant term. Hence we proceed considering only the second term. Since $\frac{\Delta}{m} + \frac{\Delta}{n} = \rho_N$, we have that $\Delta = \frac{mn}{N} \rho_N \leq N \rho_N$. Thus,

$$(14) \quad P(|I_0| \geq NH\rho_N) \lesssim \exp\left(-\gamma_N^2 \frac{N^2 \rho_N^2 mn}{N \rho_N N}\right) = \exp(-N\gamma_N^2 \Delta).$$

Case 2: If $\Delta_1 \neq \Delta_2$, then

$$\begin{aligned} & (\tilde{Z}_d(\mathbf{x}) - \tilde{Z}_d^P(\mathbf{x})) - (\tilde{Z}_d(\mathbf{x}^*) - \tilde{Z}_d^P(\mathbf{x}^*)) \\ &= \frac{1}{\sqrt{m_{\mathbf{x}} n_{\mathbf{x}}}} \left(\sum_{i,j \in A_1 \setminus B_1} (A_{ij} - \mathbb{E}_2(A_{ij})) - \sum_{i,j \in A_0 \setminus B_0} (A_{ij} - \mathbb{E}_2(A_{ij})) \right) \\ & \quad - \frac{1}{\sqrt{mn}} \left(\sum_{i,j \in B_1 \setminus A_1} (A_{ij} - \mathbb{E}_2(A_{ij})) - \sum_{i,j \in B_0 \setminus A_0} (A_{ij} - \mathbb{E}_2(A_{ij})) \right) \\ & \quad + \left(\frac{1}{\sqrt{m_{\mathbf{x}} n_{\mathbf{x}}}} - \frac{1}{\sqrt{mn}} \right) \left(\sum_{i,j \in B_1 \cap A_1} (A_{ij} - \mathbb{E}_2(A_{ij})) - \sum_{i,j \in B_0 \cap A_0} (A_{ij} - \mathbb{E}_2(A_{ij})) \right) \\ &= I_1 - I_2 + I_3. \end{aligned}$$

We directly analyze I_3 . Since $\frac{1}{\sqrt{m_{\mathbf{x}} n_{\mathbf{x}}}} - \frac{1}{\sqrt{mn}} = \frac{(\Delta_2 - \Delta_1)(m - n + \Delta_2 - \Delta_1)}{\sqrt{mn} m_{\mathbf{x}} n_{\mathbf{x}} (\sqrt{mn} + \sqrt{m_{\mathbf{x}} n_{\mathbf{x}}})}$ and notice that $(1 - \rho_N)^2 \leq m_{\mathbf{x}} n_{\mathbf{x}} / mn \leq (1 + \rho_N)^2$. By Lemma 7.1 again,

$$P(|I_3| \geq NH\rho_N) \lesssim \exp\left(-\min\left(\frac{NH\rho_N(\sqrt{mn} + \sqrt{m_{\mathbf{x}} n_{\mathbf{x}}})\sqrt{mn} m_{\mathbf{x}} n_{\mathbf{x}}}{(\Delta_2 - \Delta_1)(m - n + \Delta_2 - \Delta_1)}, \frac{H^2 \rho_N^2 mn m_{\mathbf{x}} n_{\mathbf{x}} (\sqrt{mn} + \sqrt{m_{\mathbf{x}} n_{\mathbf{x}}})^2}{\max(P)(\Delta_2 - \Delta_1)^2 (m - n + \Delta_2 - \Delta_1)^2}\right)\right).$$

Plug in $\Delta_2 - \Delta_1 \leq \rho_N n \leq \rho_N N$ and ignore some constants, we get

$$P(|I_3| \geq NH\rho_N) \lesssim \exp(-N^2 \min(H, \gamma_N^2))$$

Furthermore, $\gamma_N^2 = H \frac{H}{\max(P)} \leq 2H$, thus we have that,

$$(15) \quad P(|I_3| \geq NH\rho_N) \lesssim \exp(-N^2 \min(H, \gamma_N^2)) \leq \exp\left(-\frac{1}{2} N^2 \gamma_N^2\right).$$

I_1 and I_2 can be controlled with similar terms in (14). Combine (14) and (15), apply union bound and ignore some constants,

$$\begin{aligned} P\left(\max_{\|\mathbf{x} - \mathbf{x}^*\| \leq \delta_N} \tilde{Z}_d(\mathbf{x}) > \tilde{Z}_d(\mathbf{x}^*)\right) &\leq \sum_{\Delta_1, \Delta_2} \binom{m}{\Delta_1} \binom{n}{\Delta_2} \exp\left(-\frac{1}{2} N \gamma_N^2 (\Delta_1 + \Delta_2)\right) \\ &\leq \sum_{\Delta_1, \Delta_2} \binom{N}{\Delta_1 + \Delta_2} \exp\left(-\frac{1}{2} N \gamma_N^2 (\Delta_1 + \Delta_2)\right) \\ &\leq \sum_{\Delta=1}^{N\delta_N} \Delta \exp(\Delta - \Delta \log \Delta + \Delta \log(N) - \frac{1}{2} N \gamma_N^2 \Delta), \end{aligned}$$

where $\Delta = \Delta_1 + \Delta_2$. The last inequality uses Stirling approximation provided in Supplementary Material (Lin and Chen, 2023). Since $\Delta \geq 1$,

$$P\left(\max_{\|\mathbf{x}-\mathbf{x}^*\| \leq \delta_N} \tilde{Z}_d(\mathbf{x}) > \tilde{Z}_d(\mathbf{x}^*)\right) \leq \sum_{\Delta=1}^{N\delta_N} \Delta \left(\exp\left(1 + \log(N) - \frac{1}{2}N\gamma_N^2\right)\right)^\Delta$$

Notice that we have:

$$\lim_{N \rightarrow \infty} \sum_{\Delta=1}^{\infty} \Delta \left[\exp\left(1 + \log(N) - \frac{1}{2}N\gamma_N^2\right)\right]^\Delta = \lim_{N \rightarrow \infty} \frac{\exp\left(1 + \log(N) - \frac{1}{2}N\gamma_N^2\right)}{\left(1 - \exp\left(1 + \log(N) - \frac{1}{2}N\gamma_N^2\right)\right)^2} = 0$$

due to the condition that $\frac{N\gamma_N^2}{\log(N)} \rightarrow \infty$. This now concludes that

$$P\left(\max_{\|\mathbf{x}-\mathbf{x}^*\| \leq \delta_N} \tilde{Z}_d(\mathbf{x}) > \tilde{Z}_d(\mathbf{x}^*)\right) \rightarrow 0.$$

Together with the previous result that it will achieve weak consistency without any further assumption when the condition $\frac{N\gamma_N^2}{\log(N)} \rightarrow \infty$ hold, it now completes the proof of strong consistency of Z_d .

The proof of consistency of Z_w will be based on the consistency of Z_d . To be more specific, Step I (without re-scale factor $\frac{1}{N}$), we show that

$$(16) \quad P\left(\max_{\mathbf{x}} |\tilde{Z}_w(\mathbf{x}) - \tilde{Z}_w^P(\mathbf{x})| \geq \epsilon_N\right) \rightarrow 0.$$

Step II, we show that

$$(17) \quad \tilde{Z}_w^P(\mathbf{x}^*) - \tilde{Z}_w^P(\mathbf{x}) > 2\epsilon_N \quad \text{for } \|\mathbf{x} - \mathbf{x}^*\| \geq \delta_N \rightarrow 0$$

for δ_N satisfies that

$$\delta_N > \frac{2}{\min(\pi_1, \pi_2)} \frac{2\epsilon_N}{|P_{11} + P_{22} - P_{12} - P_{21}|}.$$

Step III, notice that

$$\begin{aligned} & P\left(\max_{\|\mathbf{x}-\mathbf{x}^*\| > \delta_N} \tilde{Z}_w(\mathbf{x}) < \tilde{Z}_w(\mathbf{x}^*)\right) \\ & \geq P\left(\max_{\|\mathbf{x}-\mathbf{x}^*\| > \delta_N} |\tilde{Z}_w(\mathbf{x}) - \tilde{Z}_w^P(\mathbf{x})| < \epsilon_N, |\tilde{Z}_w(\mathbf{x}^*) - \tilde{Z}_w^P(\mathbf{x}^*)| < \epsilon_N\right) \\ & \rightarrow 1 \quad (\text{By step I and step II}). \end{aligned}$$

Again, we provide details of obtaining (16) and (17) in Supplementary Material (Lin and Chen, 2023). Strong consistency of Z_w follows similar argument directly in Z_d case and is also put in Supplementary Material (Lin and Chen, 2023).

All the statements above are naturally for directed graphs. But we can also extend them to undirected graphs via similar treatments as in the proof of Theorem 2.3. \square

APPENDIX A: A NOTE ON MODULARITY

The original definition for modularity is (2):

$$Q = \sum_{i,j} \left(A_{ij} - \frac{k_i k_j}{2m} \right) \frac{(s_i s_j + 1)}{2}.$$

As we mentioned in Section 2.1, modularity maximization is able to capture the assortative mixing due to the fact that the observed edges inside each community are larger than their expected numbers. Similar observation holds for disassortative mixing. As we pointed out earlier, in the core-periphery case, the deviation measurement inside the core is positive and the deviation measurement inside the periphery is negative, hence cancelled out when added together. Thus, a natural idea for modifying modularity to adapt for the core-periphery structure then will be instead doing the subtraction, or the following quantity:

$$Q_d = \sum_{i,j} \left(A_{ij} - \frac{k_i k_j}{2m} \right) \delta_{ij},$$

where $\delta_{ij} = 0$ if $\mathbf{x}_i \neq \mathbf{x}_j$, $\delta_{ij} = 1$ if $\mathbf{x}_i = \mathbf{x}_j = 1$, $\delta_{ij} = -1$ if $\mathbf{x}_i = \mathbf{x}_j = 0$.

Figure 18 shows the misclassification rate of applying Q_d to the core-periphery example with connectivity matrix $P = [0.5, 0.3; 0.3, 0.1]$ for both directed graphs and undirected graphs. It clearly shows the failure of Q_d in discovering core-periphery structure since the misclassification rate is always around 0.5.

The reasons lie in the fact that while it is true that for instance, in the core, the values of A_{ij} 's are larger than their expected numbers, but the corresponding degrees k_i, k_j are also relatively large. In the meantime, the values of A_{ij} 's are smaller than their expected numbers in the periphery, but the degrees k_i, k_j are also relatively small. This is different in the case of assortative and disassortative case, resulting in the insufficient large value of deviation of Q_d at true labels assignment. Thus it is necessary for us to change the null model here or conduct other modifications in order to deal with the core-periphery structure. Our choice Z_d is certainly a successful attempt. But it is not surprising that other choices in the category for example, the weighted difference, which is the normalized version of $R_d = \frac{n-1}{N-2} R_1(\mathbf{x}) - \frac{m-1}{N-2} R_2(\mathbf{x})$, exhibits higher power than Z_d when in use since we didn't conclude Z_d to be the optimal choice in the category of discovering the core-periphery structure.

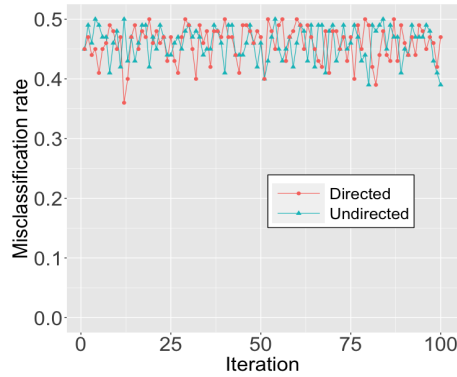


FIG 18. Misclassification rate for modified modularity under SBM with $P = [0.5, 0.3; 0.3, 0.1]$

Funding. The authors were supported in part by NSF Grants DMS-1848579 and DMS-2311399.

SUPPLEMENTARY MATERIAL

The supplementary materials contain proofs to theorems and lemmas, as well as additional numerical results.

REFERENCES

- AGGARWAL, C. C. and WANG, H. (2010). A survey of clustering algorithms for graph data. In *Managing and mining graph data* 275–301. Springer.
- AIROLDI, E. M., BLEI, D., FIENBERG, S. and XING, E. (2008). Mixed membership stochastic blockmodels. *Advances in neural information processing systems* **21**.
- AMINI, A. A., CHEN, A., BICKEL, P. J., LEVINA, E. et al. (2013). Pseudo-likelihood methods for community detection in large sparse networks. *Annals of Statistics* **41** 2097–2122.
- BAKER, D. R. (1992). A structural analysis of social work journal network: 1985-1986. *Journal of Social Service Research* **15** 153–168.
- BICKEL, P. J. and CHEN, A. (2009). A nonparametric view of network models and Newman–Girvan and other modularities. *Proceedings of the National Academy of Sciences* **106** 21068–21073.
- BORGATTI, S. P. and EVERETT, M. G. (2000). Models of core/periphery structures. *Social networks* **21** 375–395.
- CAI, T. T. and LI, X. (2015). Robust and computationally feasible community detection in the presence of arbitrary outlier nodes. *The Annals of Statistics* **43** 1027–1059.
- CHEN, H., CHEN, X. and SU, Y. (2018). A weighted edge-count two-sample test for multivariate and object data. *Journal of the American Statistical Association* **113** 1146–1155.
- CHEN, H. and FRIEDMAN, J. H. (2017). A new graph-based two-sample test for multivariate and object data. *Journal of the American statistical association* **112** 397–409.
- CHEN, Y., LI, X. and XU, J. (2018). Convexified modularity maximization for degree-corrected stochastic block models. *Annals of Statistics* **46** 1573–1602.
- CHEN, H. and LIN, X. (2023). A new clustering framework. *arXiv preprint arXiv:2305.00578*.
- FORTUNATO, S. and BARTHELEMY, M. (2007). Resolution limit in community detection. *Proceedings of the national academy of sciences* **104** 36–41.
- HOLLAND, P. W., LASKEY, K. B. and LEINHARDT, S. (1983). Stochastic blockmodels: First steps. *Social networks* **5** 109–137.
- KARRER, B. and NEWMAN, M. E. (2011). Stochastic blockmodels and community structure in networks. *Physical review E* **83** 016107.
- KRZAKALA, F., MOORE, C., MOSSEL, E., NEEMAN, J., SLY, A., ZDEBOROVÁ, L. and ZHANG, P. (2013). Spectral redemption in clustering sparse networks. *Proceedings of the National Academy of Sciences* **110** 20935–20940.
- LEICHT, E. A. and NEWMAN, M. E. (2008). Community structure in directed networks. *Physical review letters* **100** 118703.
- LI, T., LEI, L., BHATTACHARYYA, S., VAN DEN BERGE, K., SARKAR, P., BICKEL, P. J. and LEVINA, E. (2022). Hierarchical community detection by recursive partitioning. *Journal of the American Statistical Association* **117** 951–968.
- LIN, X. and CHEN, H. (2023). Supplement to “UBSEA: A Unified Community Detection Framework”.
- LIU, Y.-W. and CHEN, H. (2022). A fast and efficient change-point detection framework based on approximate k-nearest neighbor graphs. *IEEE Transactions on Signal Processing*.
- MALLIAROS, F. D. and VAZIRGIANNIS, M. (2013). Clustering and community detection in directed networks: A survey. *Physics reports* **533** 95–142.
- MOORE, C., YAN, X., ZHU, Y., ROUQUIER, J.-B. and LANE, T. (2011). Active learning for node classification in assortative and disassortative networks. In *Proceedings of the 17th ACM SIGKDD international conference on Knowledge discovery and data mining* 841–849.
- NEPUSZ, T., PETRÓCZI, A., NÉGYESSY, L. and BAZSÓ, F. (2008). Fuzzy communities and the concept of bridgeness in complex networks. *Physical Review E* **77** 016107.
- NEWMAN, M. E. (2002). Assortative mixing in networks. *Physical review letters* **89** 208701.
- NEWMAN, M. E. (2003a). Mixing patterns in networks. *Physical review E* **67** 026126.

- NEWMAN, M. E. (2003b). The structure and function of complex networks. *SIAM review* **45** 167–256.
- NEWMAN, M. E. (2006a). Modularity and community structure in networks. *Proceedings of the national academy of sciences* **103** 8577–8582.
- NEWMAN, M. E. (2006b). Finding community structure in networks using the eigenvectors of matrices. *Physical review E* **74** 036104.
- NEWMAN, M. E. and GIRVAN, M. (2004). Finding and evaluating community structure in networks. *Physical review E* **69** 026113.
- NEWMAN, M. E. and LEICHT, E. A. (2007). Mixture models and exploratory analysis in networks. *Proceedings of the National Academy of Sciences* **104** 9564–9569.
- PEIXOTO, T. P. (2018). Nonparametric weighted stochastic block models. *Physical Review E* **97** 012306.
- QIN, T. and ROHE, K. (2013). Regularized spectral clustering under the degree-corrected stochastic blockmodel. *Advances in neural information processing systems* **26**.
- REICHARDT, J. and BORNHOLDT, S. (2006). Statistical mechanics of community detection. *Physical review E* **74** 016110.
- VON LUXBURG, U. (2007). A tutorial on spectral clustering. *Statistics and computing* **17** 395–416.
- WANG, Y. R. and BICKEL, P. J. (2017). Likelihood-based model selection for stochastic block models. *The Annals of Statistics* **45** 500–528.
- ZHANG, X., MARTIN, T. and NEWMAN, M. E. (2015). Identification of core-periphery structure in networks. *Physical Review E* **91** 032803.
- ZHAO, Y., LEVINA, E. and ZHU, J. (2012). Consistency of community detection in networks under degree-corrected stochastic block models. *The Annals of Statistics* **40** 2266–2292.